Supplementary Information for:

Electrocatalysis at Organic-Metal Interfaces: Identification of Structure-Reactivity Relationships for CO_2 Reduction at Modified Cu Surfaces

Aya K. Buckley,[1,2] *Michelle Lee,*[1,3] *Tao Cheng,*[4,5] *Roman V. Kazantsev,*[1,2] *David M. Larson,*[1] *William A. Goddard III,*[4] *F. Dean Toste*[1,2] *and Francesca M. Toma*[1]

[1] Joint Center for Artificial Photosynthesis and [2] Chemical Sciences Division, Lawrence Berkeley National Laboratory, 1 Cyclotron Road, Berkeley, CA 94720 USA.

[2] Department of Chemistry, University of California, Berkeley, CA 94720, USA.

[3] Department of Chemistry and Chemical Biology, Cornell University, Ithaca, NY 14853, USA.

[4] Joint Center for Artificial Photosynthesis and Materials and Process Simulation Center, California Institute of Technology, Pasadena, CA 91125, USA.

[5] Institute of Functional Nano & Soft Materials (FUNSOM), Jiangsu Key Laboratory for Carbon-Based Functional Materials & Devices, Joint International Research Laboratory of Carbon-Based Functional Materials and Devices, Soochow University, 199 Ren'ai Road, Suzhou, 215123, Jiangsu, PR China

Table of Contents

SA. Experimental methods

Materials: All chemicals were obtained from commercial suppliers and used without further purification, unless otherwise noted. Copper foil (0.254 mm thick, 99.9%) was purchased from Alfa Aesar and cut with a bench shear into 2 cm x 3 cm electrodes before use. Carbon dioxide (99.995%) and nitrogen (99.999%) were obtained from Praxair. Nafion 117 solution (~5% in a mixture of lower aliphatic alcohols and water), polyvinylpyrrolidone (average MW 40,000), polyallylamine (average MW 17,000, 20 wt% in water), polyvinyl alcohol (MW 89,000-98,000, 99+% hydrolyzed), polyethylene glycol (average MW 20,000), polystyrene (average MW 192,000), didecyldimethylammonium bromide (98%), dihexadecyldimethylammonium bromide (97%), tetrahexadecylammonium bromide (98%), and trihexyltetradecylphosphonium bromide (95%) were purchased from Sigma-Aldrich. Cetyltrimethylammonium bromide (98%) was obtained from Spectrum Chemical. Selemion AMV anion-exchange membrane was purchased from AGC Engineering Co., LTD.

Instrumentation: Gas chromatography (GC) data was collected on a multiple gas analyzer #5 from SRI Instruments. High performance liquid chromatography (HPLC) was performed with an UltiMate 3000 HPLC from Thermo Fisher Scientific. ^{1}H NMR data was collected on an Ascend 500 MHz NMR from Bruker. Contact angle measurements were performed with a VCA Optima instrument from AST Products.

Electrochemical Methods:
Electrochemical experiments: Electrochemical experiments were conducted in a two-compartment flow cell fabricated from PEEK following a reported design.[1] A Selemion AMV anion-exchange membrane separated the two chambers. A Pt foil was used as the counter electrode.

A Leak-Free Ag/AgCl electrode (LF-1, 1.0 mm outer diameter, Innovative Instruments, Inc.) was used as the reference electrode. The reference electrode was calibrated against a second reference electrode, which in turn was calibrated in a two-electrode system with H_2 bubbled over a Pt wire as the counter electrode and a 1M H_2SO_4 solution as the electrolyte.

The applied potentials were converted from Ag/AgCl scale to the RHE scale via the equation: $E_{RHE} = E_{Ag/AgCl} + 0.197 + 0.059*pH$, where the pH used is the bulk pH for the CO_2-saturated electrolyte (6.8).

Electrochemical experiments:
Electrolyte preparation: Potassium carbonate solution (0.05M) was prepared from high purity potassium carbonate (99.995%, Sigma Aldrich) and water from a Milli-Q Water Purification System (resistivity of 18.2 MΩ-cm, Millipore). The solution was saturated with CO_2 for a minimum of 10 minutes within the experimental cell setup immediately prior to all electrochemical experiments.

Preparation of functionalized samples: The Cu foils were prepared as described in the Methods section of the main text, and the functionalized samples were prepared as described below:

Polyvinylpyrrolidone (**1**) *and polyallylamine* (**3**): 10 mg of polymer was dissolved in iPrOH (1 mL), and 100 µL of this solution was dropcast onto the Cu foil. Once dry, 100 µL of Nafion solution (10 µL of commercial Nafion solution in 1 mL iPrOH) was dropcast onto the Cu surface.

Tetrahexadecylammonium bromide (**2**): 5 mg of ammonium salt was suspended in iPrOH (5 mL) and heated briefly at 60˚C to dissolve. 100 µL of this solution was dropcast onto the Cu foil. Once dry, 100 µL of Nafion solution (5 µL of commercial Nafion solution in 5 mL iPrOH) was dropcast onto the Cu surface.

Polystyrene (**4**): 10 mg of polymer was dissolved in toluene (1 mL), and 100 µL of this solution was dropcast onto the Cu foil. Once dry, 100 µL of Nafion solution (10 µL of commercial Nafion solution in 1 mL iPrOH) was dropcast onto the Cu surface.

Polyvinyl alcohol (**5**): 10 mg of polymer was suspended in water (400 µL) and heated to 70˚C to dissolve. An additional 600 µL of MeOH was added to the solution. 100 µL of this solution was dropcast onto the Cu foil. Once dry, 100 µL of Nafion solution (10 µL of commercial Nafion solution in 1 mL iPrOH) was dropcast onto the Cu surface.

Polyethylene glycol (**6**): 10 mg of polymer was suspended in MeOH (1 mL) and heated briefly at 60˚C to dissolve. 100 µL of this solution was dropcast onto the Cu foil. Once dry, 100 µL of Nafion solution (10 µL of commercial Nafion solution in 1 mL iPrOH) was dropcast onto the Cu surface.

Trihexyltetradecylphosphonium bromide (**7**), *dihexadecyldimethylammonium bromide* (**8**), *didecyldimethylammonium bromide* (**9**) *and cetyltrimethylammonium bromide* (**10**): 0.0274 mmol of the organic species was dissolved in iPrOH (1 mL), and 100 µL of this solution was dropcast onto the Cu foil. Once dry, 100 µL of Nafion solution (1 µL of commercial Nafion solution per mg of organic species added to 1 mL iPrOH) was dropcast onto the Cu surface.

SB. Experiments with Nafion

Cu surfaces were tested with Nafion in the absence of other modifiers to evaluate whether Nafion on its own influenced the product selectivity. The data below, collected at the lowest and highest loadings of Nafion employed in the main manuscript, suggest that Nafion does not affect CO2R selectivity of Cu.

Table S1. Faradaic efficiencies and total current of Ox Cu and Cu functionalized solely with Nafion at varying loadings. Reported values are averages from at least three trials.

	H_2	CO	Formic Acid	Other	Total FE	Total Current (mA/cm^2)
Ox Cu	28%	28%	34%	6%	96%	0.73
1 µL Nafion per mL iPrOH[a]	27%	30%	31%	5%	93%	0.75
10 µL Nafion per mL iPrOH[b]	29%	31%	30%	4%	95%	0.80
15.8 µL Nafion per mL iPrOH[c]	27%	29%	30%	4%	90%	0.82

[a]5 µL Nafion was dissolved in 5 mL iPrOH. 100 µL of this solution was dropcast onto oxide-derived Cu. This loading is the same as for experiments with **2**- the lowest loading of Nafion used for the figures in the main manuscript. [b]10 µL Nafion was dissolved in 1 mL iPrOH. 100 uL of this solution was dropcast onto oxide-derived Cu. [c]15.8 µL Nafion was dissolved in 1 mL iPrOH. 100 µL of this solution was dropcast onto oxide-derived Cu. This loading is the same as for experiments with **8**- the highest loading of Nafion used for the figures in the main manuscript.

In addition, experiments with modifiers **8** and **9** were conducted with and without Nafion to evaluate the role of the binder.

Chronoamperometry traces collected with Nafion were less noisy than traces without Nafion (**Fig. S1**). Furthermore, in the absence of Nafion, the electrolyte was observed to bubble more vigorously out of the cell, particularly in studies with more hydrophilic species. This observation suggests that in the absence of Nafion, the modifiers dissolve more readily in the electrolyte and yield a soapy solution. Therefore, Nafion was applied in all of the studies in the main manuscript at a loading of 1 µL Nafion per mg of modifier.

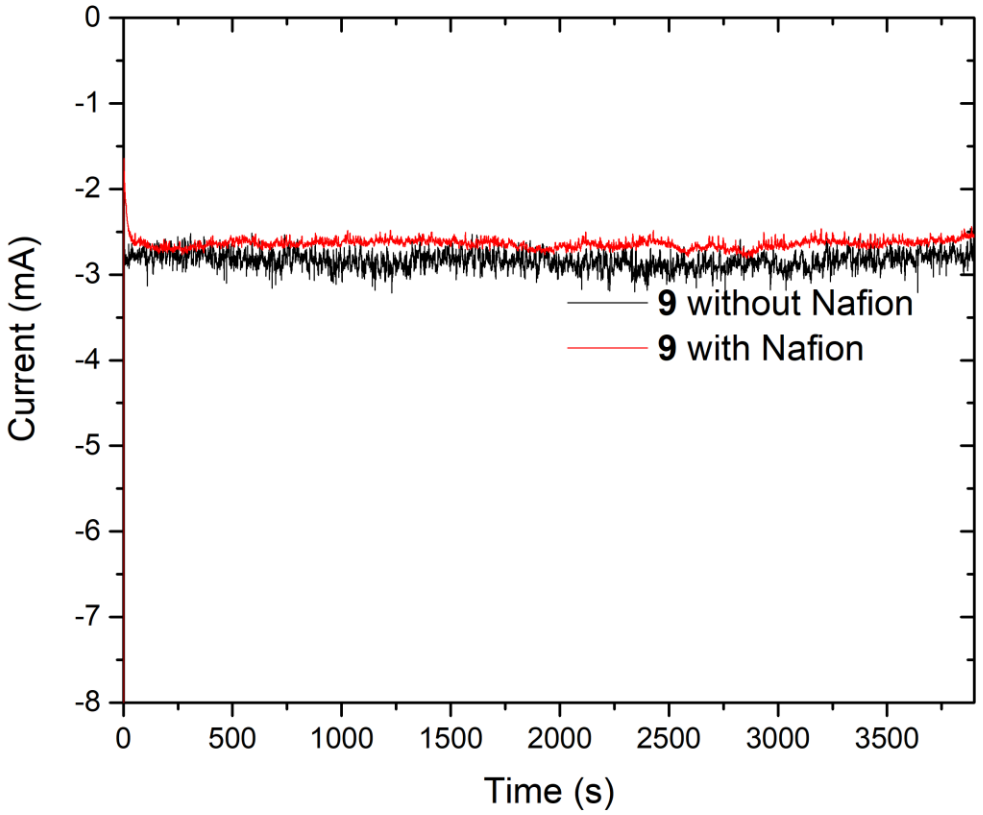

Figure S1. Chronoamperometry of Cu modified with 9, both with and without Nafion binder. In the presence of Nafion, the CA trace appears less noisy than in the absence of Nafion. Therefore, Nafion binder was employed as a binder for the experiments in the text. CA in the above figure was conducted at -0.7 V vs. RHE as described in the Experimental Methods.

The product distribution for these experiments without Nafion demonstrated the same trend as experiments with Nafion: **8** yielded more CO than the unfunctionalized surface, while **9** yielded more formic acid.

Table S2. Faradaic efficiency data with and without Nafion with 8

	H_2	CO	Formic Acid	Other	Total FE	Total Current (mA/cm^2)
with Nafion	3%	76%	18%	0	97%	0.31
no Nafion	7%	63%	31%	0	101%	0.34

Table S3. Faradaic efficiency data with and without Nafion with 9

	H_2	CO	Formic Acid	other	Total FE	Total Current (mA/cm^2)
with Nafion	21%	8%	62%	0	91%	2.45
no Nafion	21%	6%	73%	0	100%	2.84

SC. Chronoamperometry traces

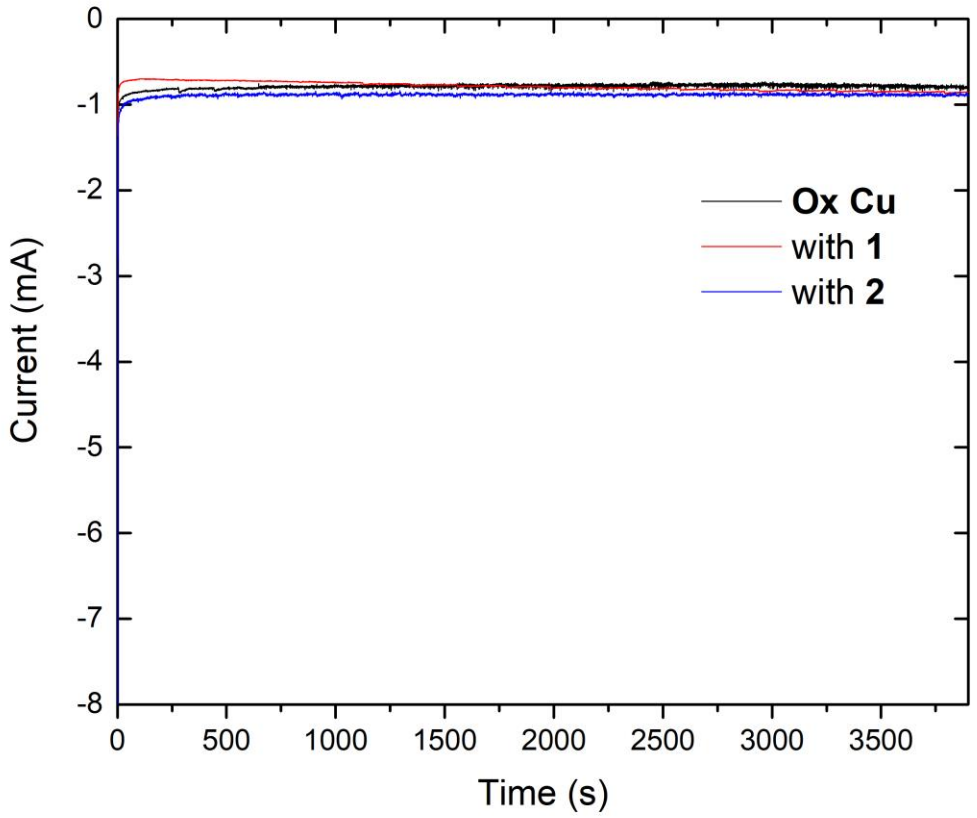

Figure S2. Chronoamperometry traces for Ox Cu and experiments with 1 and 2. Chronoamperometry traces indicate that for experiments with **Ox Cu**, **1** and **2**, the currents remain stable over the course of the 65-minute experiment. The total current is also similar for the three traces, suggesting that mass transfer of CO_2 and protons is not substantially inhibited by the presence of the modifiers.

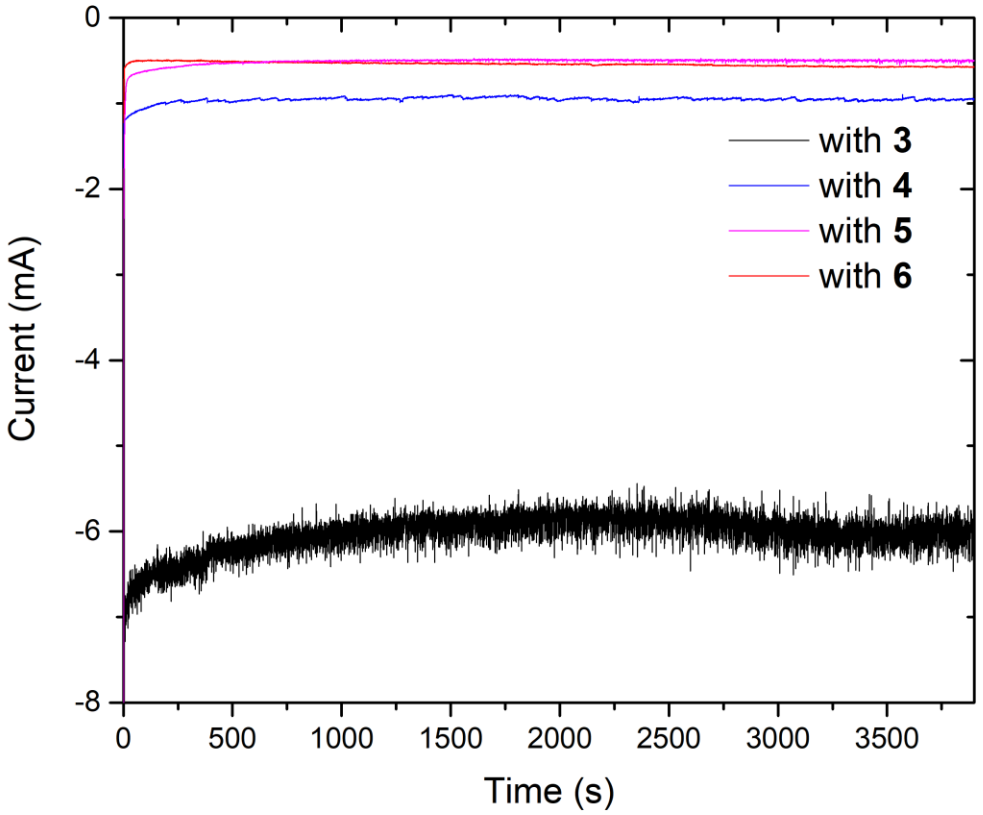

Figure S3. **Chronoamperometry traces of neutral polymers as modifiers on Cu.** CA traces indicate that the currents remain stable over the course of the 65-minute experiment.

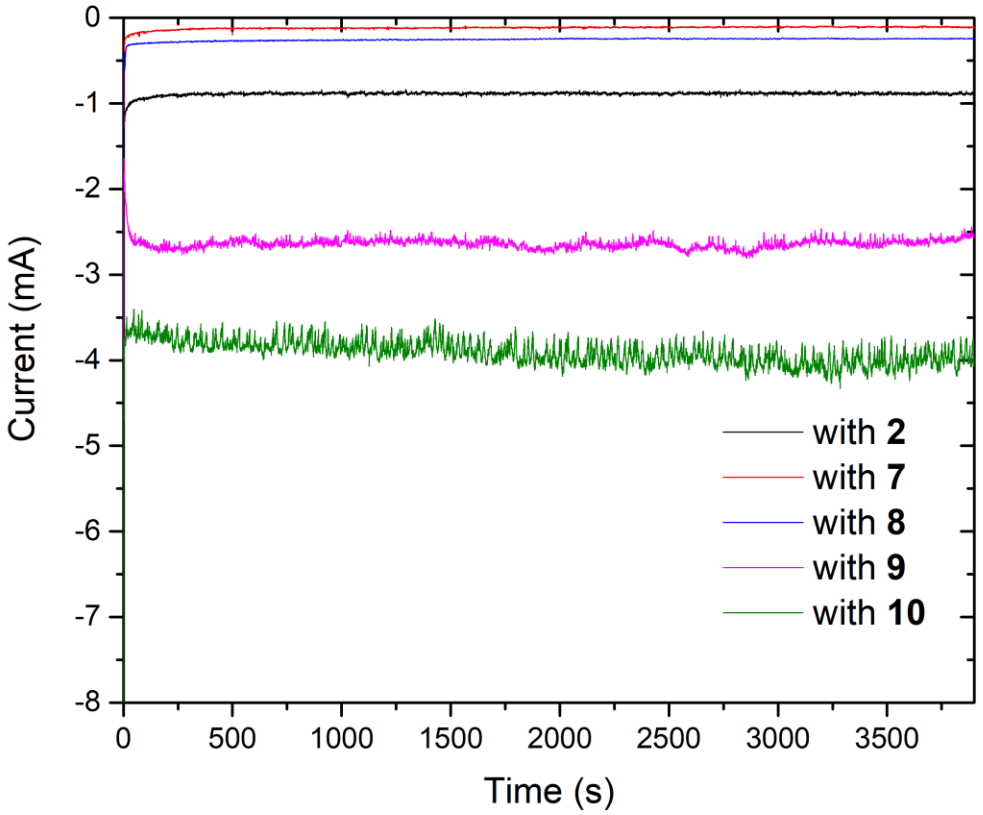

Figure S4. **Chronoamperometry traces of cationic molecules as modifiers on Cu**. CA traces indicate that the currents remain stable over the course of the 65-minute experiment.

SD. Experiments with varying amounts of modifier

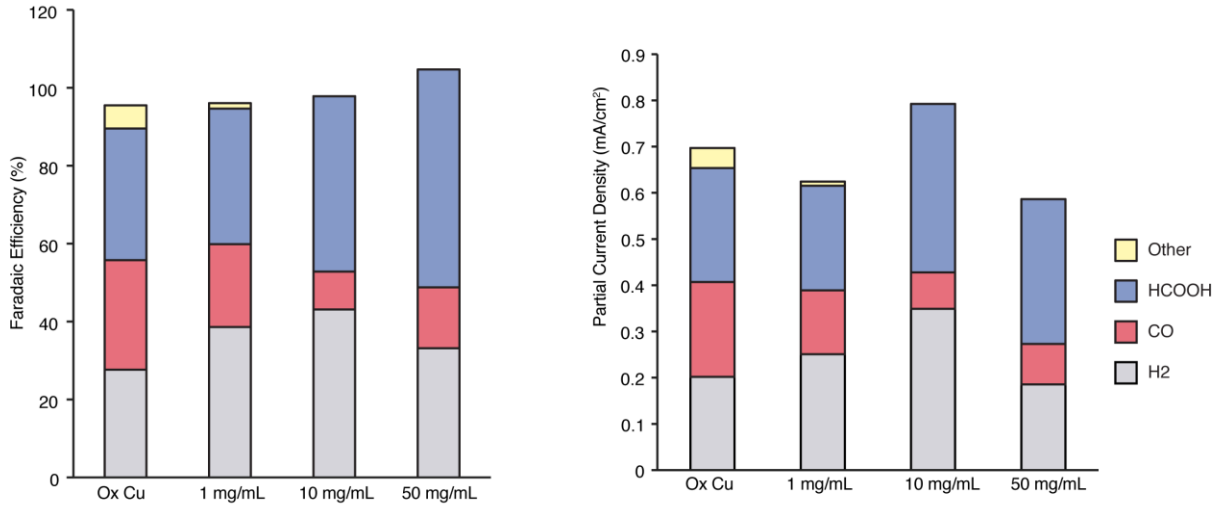

Figure S5. **Experiments with varying loadings of polyvinylpyrrolidone (1).** Solutions of 1, 10 and 50 mg of **1** in 1 mL iPrOH were prepared, and 100 µL of this solution were dropcast onto oxide-derived copper surfaces as previously described. Once dry, 1, 10, and 50 µL of Nafion, respectively, were then dissolved in iPrOH, and 100 µL of this solution was dropcast onto the Cu surface. The product distribution was characterized as described in the Experimental Methods.

As compared to **Ox Cu**, which yields 34% formic acid, the selectivity increases to 35%, 45% and 56% formic acid with increasing loadings of **1**. We hypothesize that the lowest loading is too low to have a substantial effect on the product selectivity. In terms of partial current density, the amount of formic acid generated with **Ox Cu** (0.25 mA/cm^2) changes to 0.23, 0.36 and 0.31 mA/cm^2 with the 1, 10 and 50 mg/mL solutions, respectively.

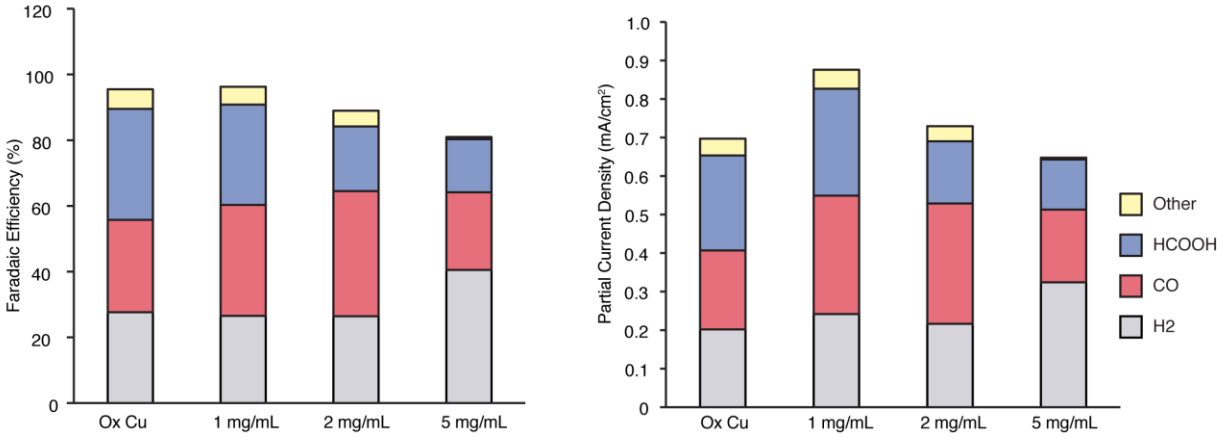

Figure S6. **Experiments with varying loadings of tetrahexadecylammonium bromide (2)**. Solutions of 1, 2 and 5 mg of **2** per 1 mL iPrOH were prepared, and 100 µL of this solution were dropcast onto oxide-derived copper surfaces as previously described. Once dry, 1, 2, and 5 µL of Nafion, respectively, were then dissolved per mL of iPrOH, and 100 µL of this solution was dropcast onto the Cu surface. The product distribution was characterized as described in the Experimental Methods.

As compared to **Ox Cu**, which yields 28% CO, the addition of **2** yields 34% and 38% CO with 1 and 2 mg/mL stock solutions, respectively. With a stock solution of 5 mg/mL, the selectivity for CO drops to 24%, and the total FE also drops to 81%. We observed in this experiment that the thick layer of modifier had partially peeled off of the electrode, and this mechanical instability may have affected the ability to close the FE gap. In terms of partial current density, the amount of CO generated with **Ox Cu** (0.21 mA/cm^2) changes to 0.31, 0.31 and 0.19 mA/cm^2 with the addition of 1, 2 and 5 mg/mL stock solutions, respectively.

SE. Product distribution at more negative potentials

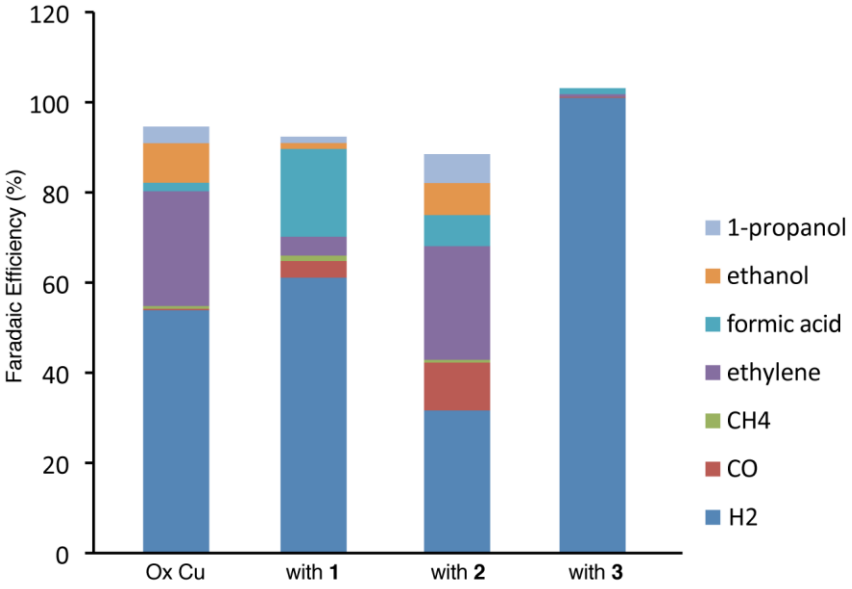

Figure S7. CO_2 reduction conducted at -1.0 V vs. RHE. The experiment was conducted as previously described, except at -1.0 V vs. RHE instead of -0.7 V vs. RHE, for **Ox Cu** and surfaces modified with **1**, **2**, and **3**.

SF. Experiments under N_2

The substrates that demonstrated enhanced selectivity for CO2R products were also examined under N_2. Experiments under N_2 were conducted with the same process, loadings and conditions as conducted for the data in **Fig. 1**, except with N_2 flow instead of CO_2. Faradaic efficiencies and total current for these trials are reported below. CO2R activity disappears, indicating that the selectivities observed in **Fig. 1** originate from CO2R, and not from decomposition of the modifier. The low FE for H_2 and low total FE observed with **8** is due to the low total current, which would yield an amount of H_2 that is close to the detection limit of our instrument.

Table S4. Functionalized Cu under N_2.

	H_2	CO	Formic Acid	other	Total FE	Total Current (mA/cm^2)
Ox Cu-under N_2	108.2%	0.2%	0%	0%	108.4%	0.41
With **1** under N_2	115.0%	0.1%	0%	0%	115.0%	0.57
With **2** under N_2	113.4%	0%	0%	0%	113.4%	0.31
With **6** under N_2	113.9%	0.2%	0%	0%	114.1%	0.20
With **7** under N_2	108.5%	0.1%	0%	0%	108.6%	0.12
With **8** under N_2	31.6%	0.7%	0%	0%	32.3%	0.03
With **9** under N_2	117.5%	0.2%	1.6%	0%	119.3%	0.35
With **10** under N_2	109.6%	0%	0%	0%	109.6%	0.47

SG. NMR characterization of modifiers and electrolyte

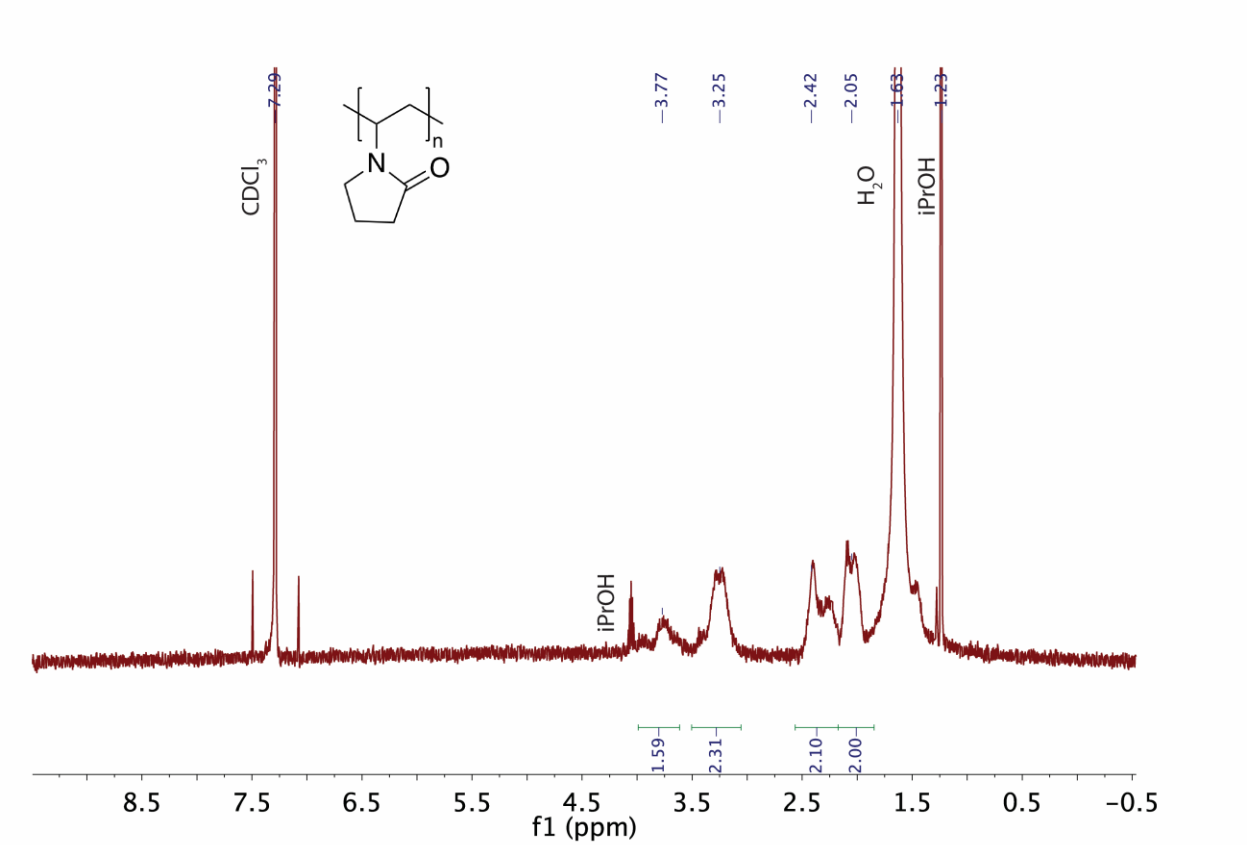

Figure S8. ^{1}H NMR of polyvinylpyrrolidone (**1**), rinsed from electrode after 65 minutes of chronoamperometry.

The CA experiment was conducted as described in the Experimental Methods, except with an increase in the loading. A 50 mg sample of polyvinylpyrrolidone (**1**) was dissolved in 1 mL iPrOH, and 100 µL of this solution was dropcast onto the oxide-derived Cu surface. 50 µL of Nafion solution was dissolved in 1 mL of iPrOH, and 100 µL of the Nafion solution was then dropcast onto the functionalized Cu surface.

^{1}H NMR (500 MHz, $CDCl_3$, ppm): δ 3.77 (m, 1H), 3.25 (m, 2H), 2.42 (m, 2H), 2.05 (m, 2H), 1.63 (m, 2H).

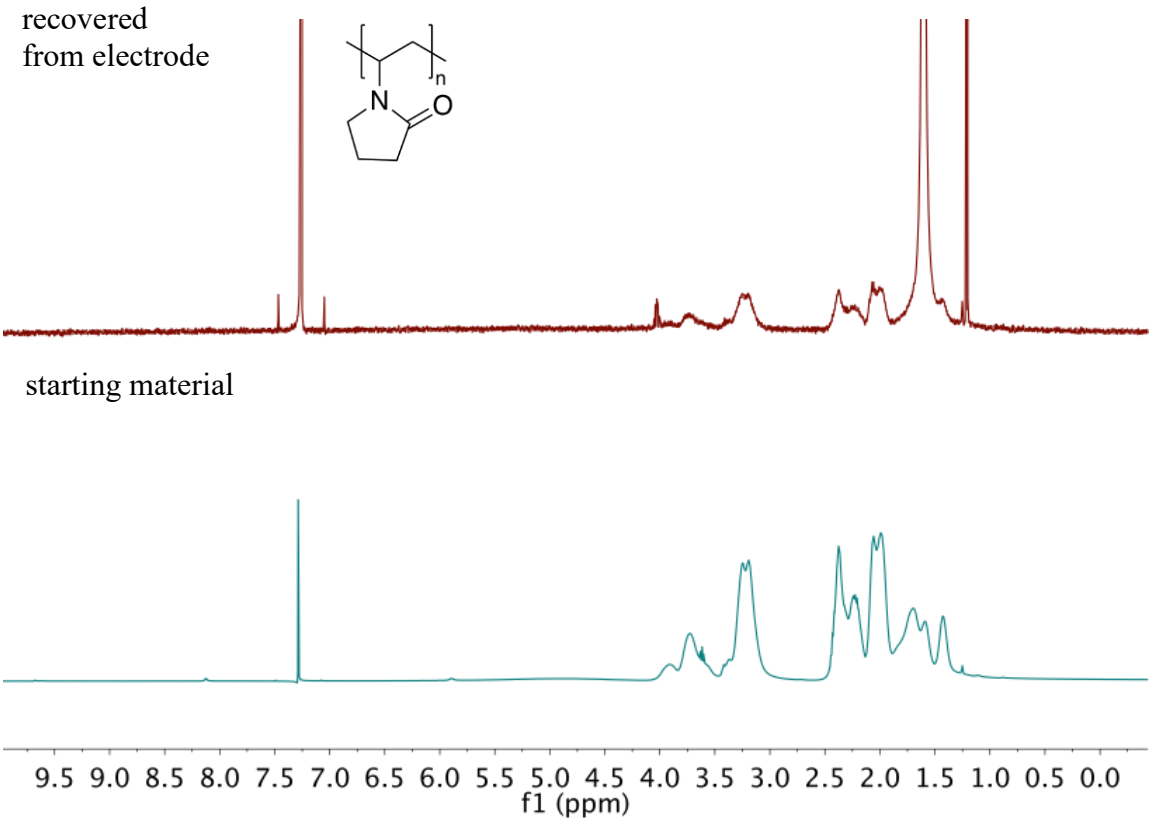

Figure S9. ^{1}H NMR of commercial polyvinylpyrrolidone (**1**) in $CDCl_3$ (bottom), compared with rinse of electrode after 65 minutes of chronoamperometry, also in $CDCl_3$ (top).

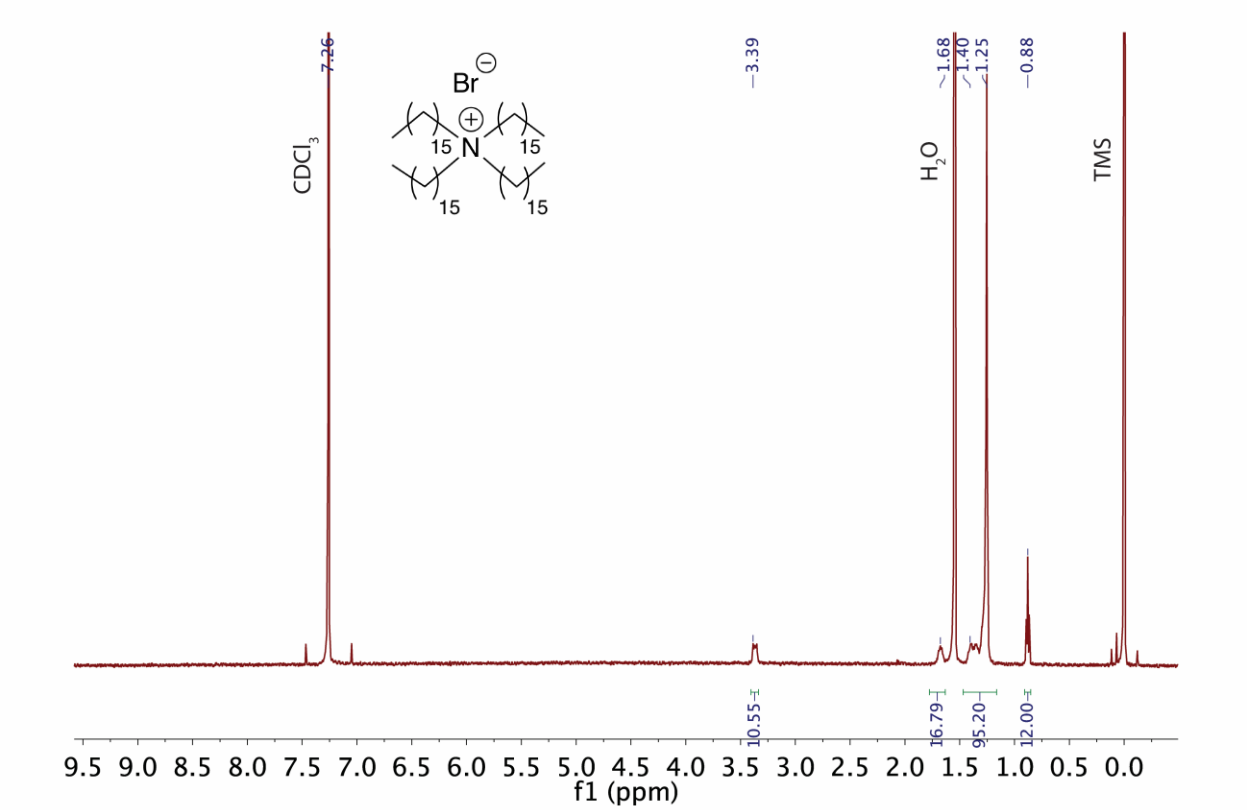

Figure S10. ^{1}H NMR of tetrahexadecylammonium bromide (**2**), rinsed from electrode after 65 minutes of chronoamperometry.

The CA experiment was conducted as described in the Experimental Methods, except with an increase in the loading. A 3 mg sample of (**2**) was dissolved in 1 mL iPrOH at 60 ˚C, and 100 µL of this solution was dropcast onto the oxide-derived Cu surface. 3 µL of Nafion solution was dissolved in 1 mL of iPrOH, and 100 µL of the Nafion solution was then dropcast onto the functionalized Cu surface.

^{1}H NMR (500 MHz, $CDCl_3$, ppm): δ 3.39 (m, 8H), 1.68 (m, 16H), 1.25 (m, 96H), 0.88 (t, *J* = 6.80, 12H).

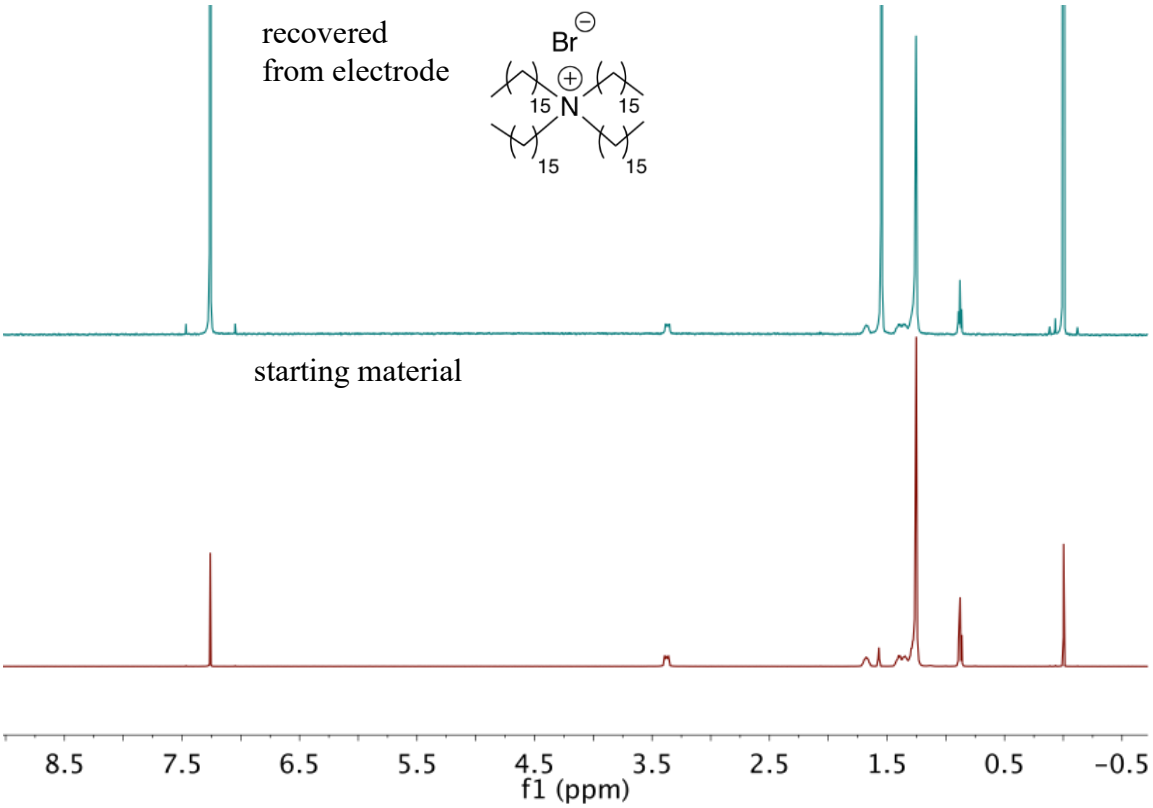

Figure S11. ^{1}H NMR of commercial tetrahexadecylammonium bromide (**2**) in $CDCl_3$ (bottom), compared with rinse of electrode after 65 minutes of chronoamperometry, also in $CDCl_3$ (top).

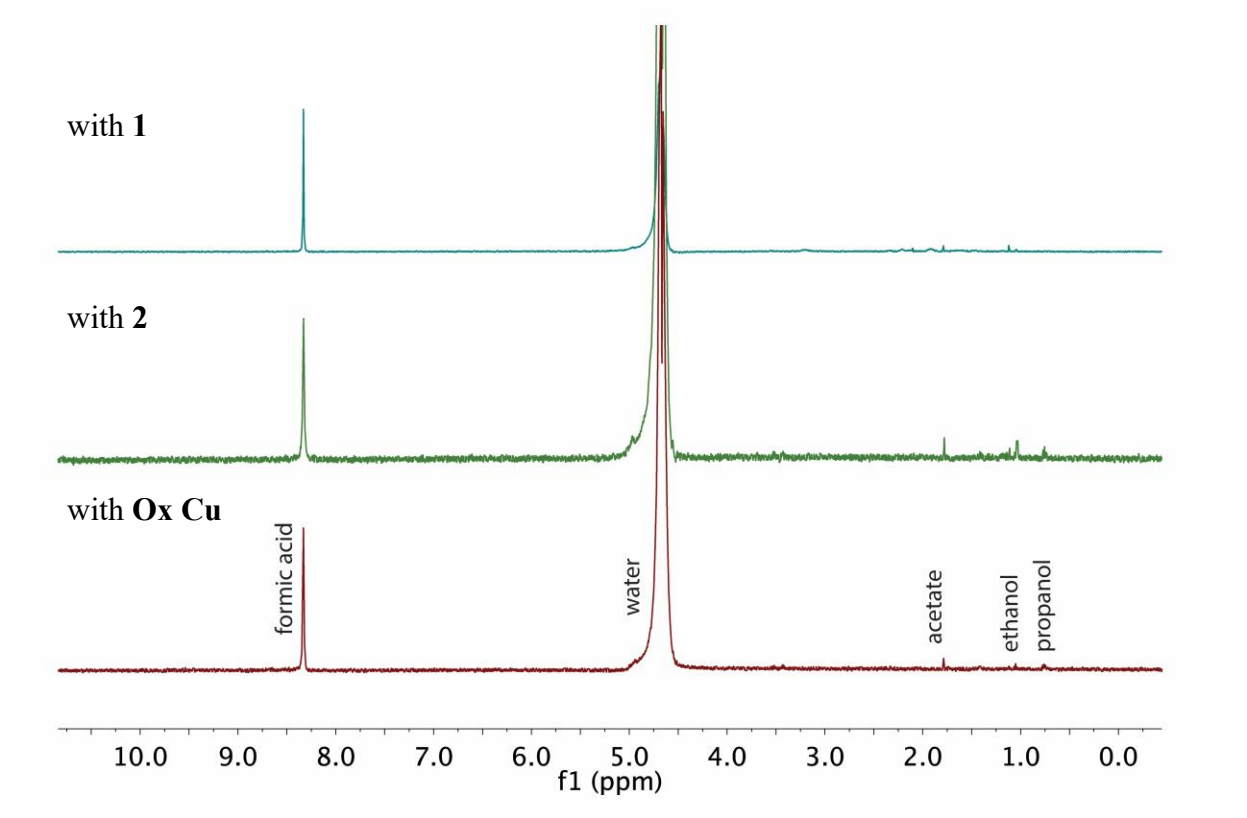

Figure S12. ^{1}H NMR of catholyte with suppression of the water peak, from bottom to top: a) reaction with Ox Cu, b) reaction with tetrahexadecylammonium bromide (**2**), c) reaction with polyvinylpyrrolidone (**1**). The spectra indicate the presence of formic acid and traces of other products; the absence of additional products, in conjunction with **Figures S8-11**, suggests that the modifiers remain intact throughout the experiment. The spectra were collected with 700 µL of catholyte and 35 µL of D_2O.

Catholyte samples were collected from the same experiments reported in **Fig 1**.

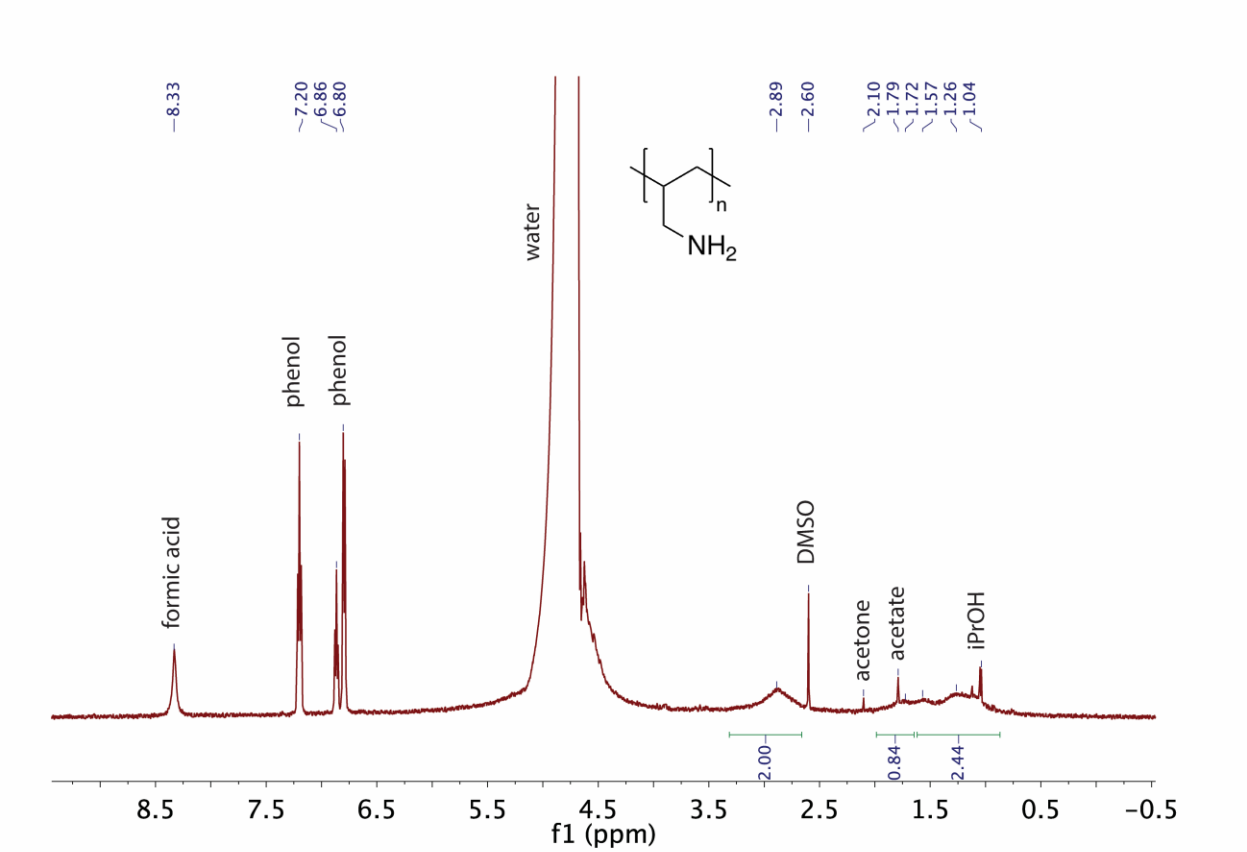

Figure S13. ^{1}H NMR of polyallylamine (**3**) from catholyte. Spectrum was collected using suppression of the water peak, and phenol and DMSO were added as internal standards.

The CA experiment was conducted as described in the Experimental Methods, except with an increase in the loading. A 50 mg sample of polyallylamine (**3**) was dissolved in 1 mL iPrOH, and 100 µL of this solution was dropcast onto the oxide-derived Cu surface. 50 µL of Nafion solution was dissolved in 1 mL of iPrOH, and 100 µL of the Nafion solution was then dropcast onto the functionalized Cu surface.

^{1}H NMR (500 MHz, H_2O and D_2O, ppm): δ 2.89 (m, 2H), 1.79 (m, 1H), 1.26 (m, 2H).

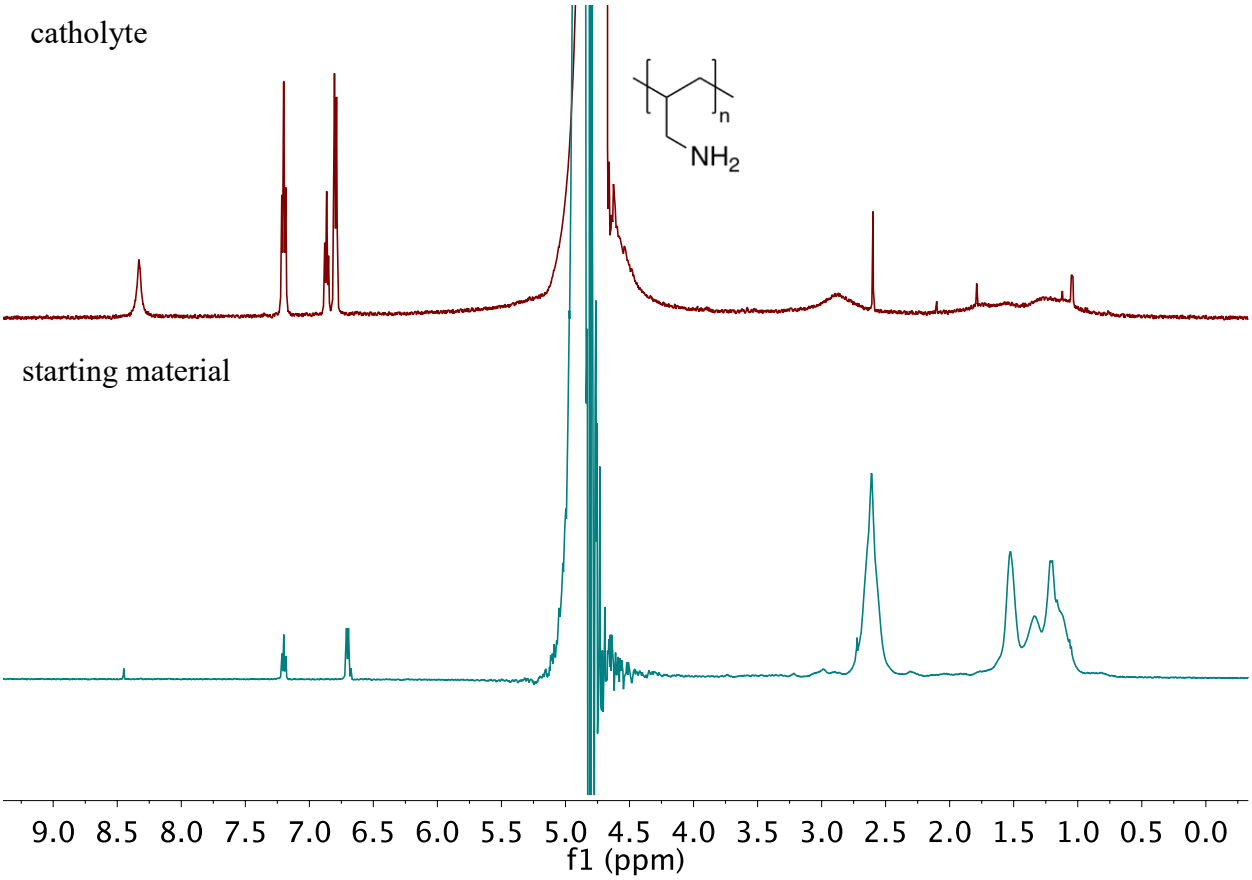

Figure S14. ^{1}H NMR of commercial polyallylamine (**3**) in H_2O and D_2O (bottom), compared with electrolyte after 65 minutes of chronoamperometry, also in H_2O and D_2O (top). Spectrum was collected using suppression of the water peak, and phenol and DMSO were added as internal standards.

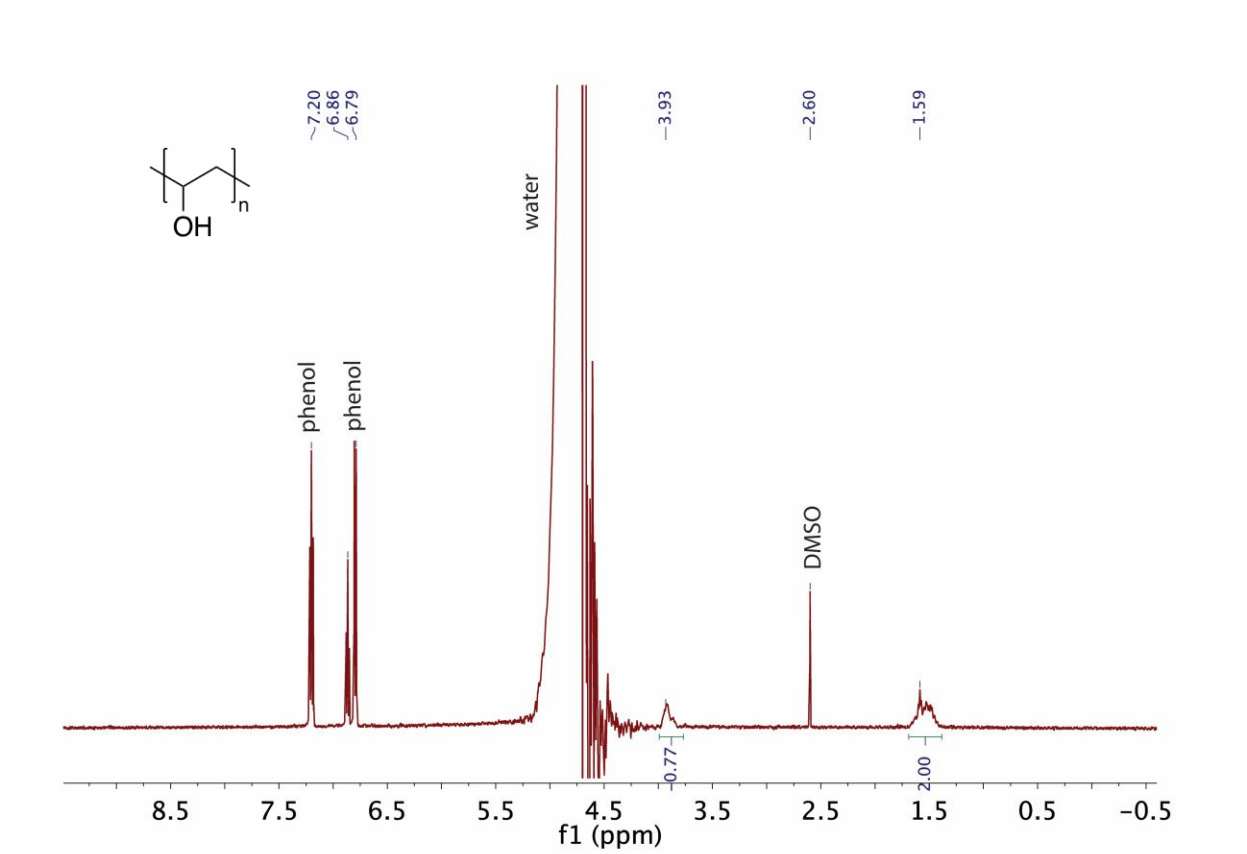

Figure S15. ^{1}H NMR of polyvinyl alcohol (**5**), rinsed from electrode after 65 minutes of chronoamperometry. Spectrum was collected using suppression of the water peak, and phenol and DMSO were added as internal standards.

The CA experiment was conducted as described in the Experimental Methods using the same loadings.

^{1}H NMR (500 MHz, H_2O and D_2O, ppm): δ 3.93 (m, 1H), 1.59 (m, 2H), (proton of –OH cannot be seen because it overlapped with water peak).

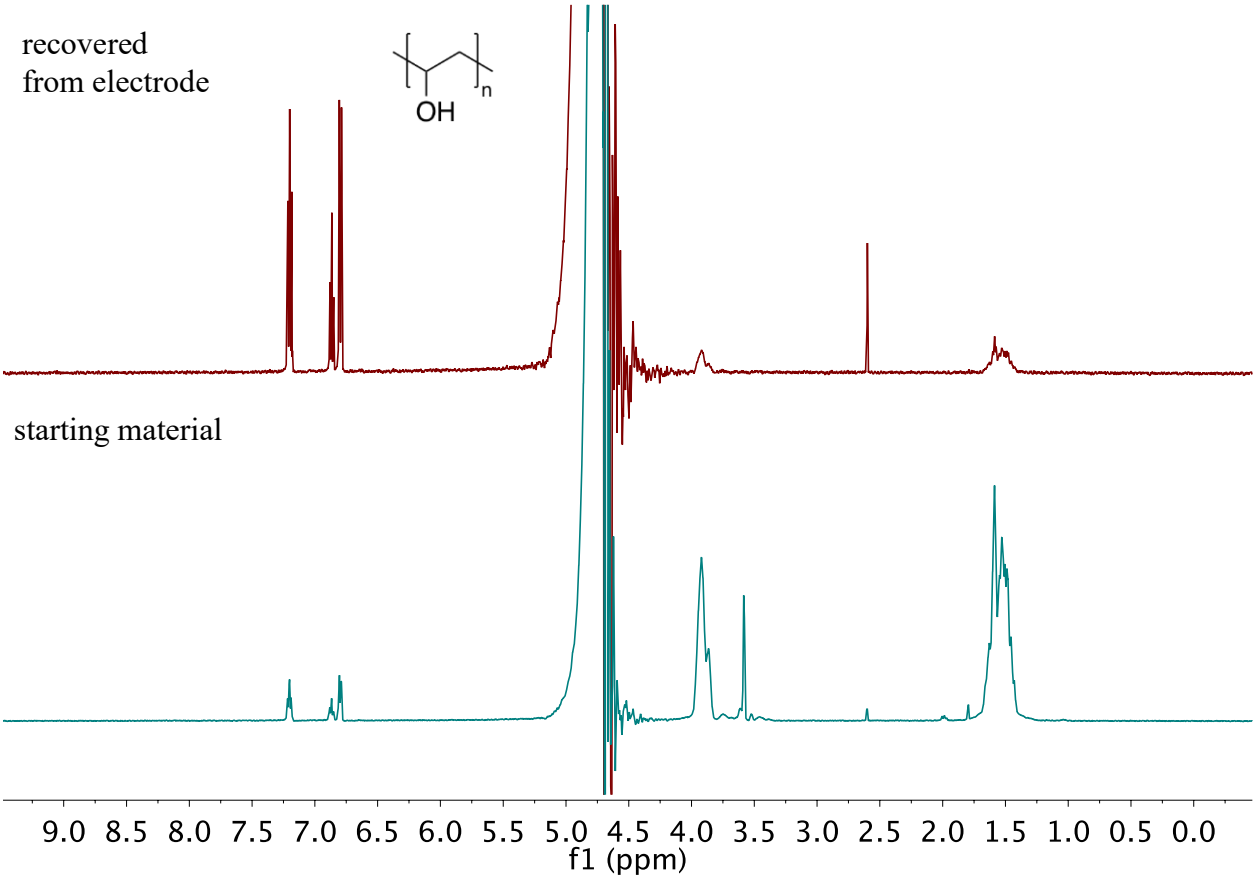

Figure S16. ^{1}H NMR of commercial polyvinyl alcohol in a mixture of H_2O and D_2O (**5**), compared with rinse of electrode after 65 minutes of chronoamperometry in the same solvent system. Spectra were collected using suppression of the water peak, and phenol and DMSO were added as internal standards.

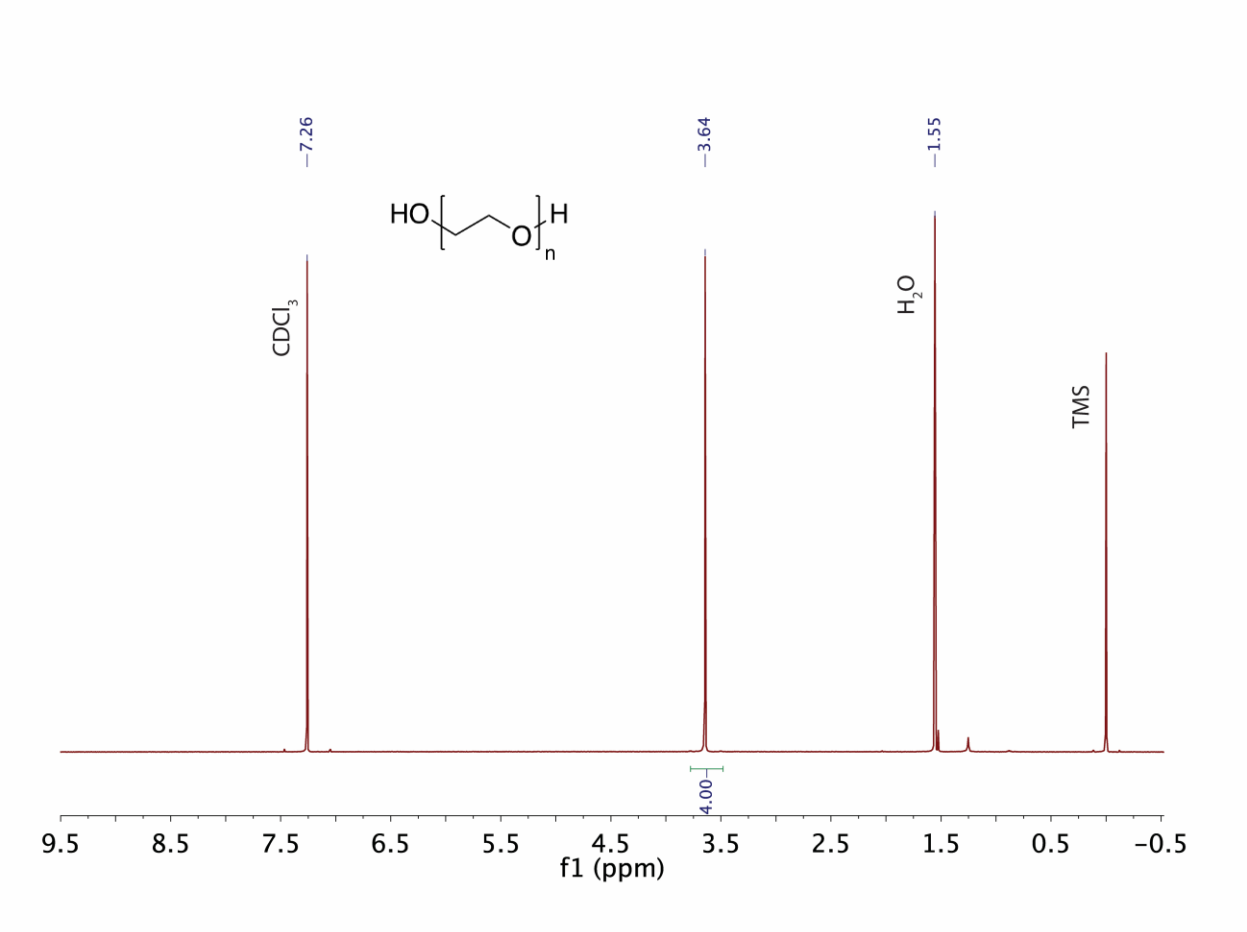

Figure S17. ^{1}H NMR of polyethylene glycol (**6**), rinsed from electrode after 65 minutes of chronoamperometry.

The CA experiment was conducted as described in the Experimental Methods, except with an increase in the loading. A 50 mg sample of polyethylene glycol (**6**) was dissolved in 1 mL MeOH at 60˚C, and 100 µL of this solution was dropcast onto the oxide-derived Cu surface. 50 µL of Nafion solution was dissolved in 1 mL of iPrOH, and 100 µL of the Nafion solution was then dropcast onto the functionalized Cu surface.

^{1}H NMR (500 MHz, $CDCl_3$, ppm): δ 3.64 (s, 4H).

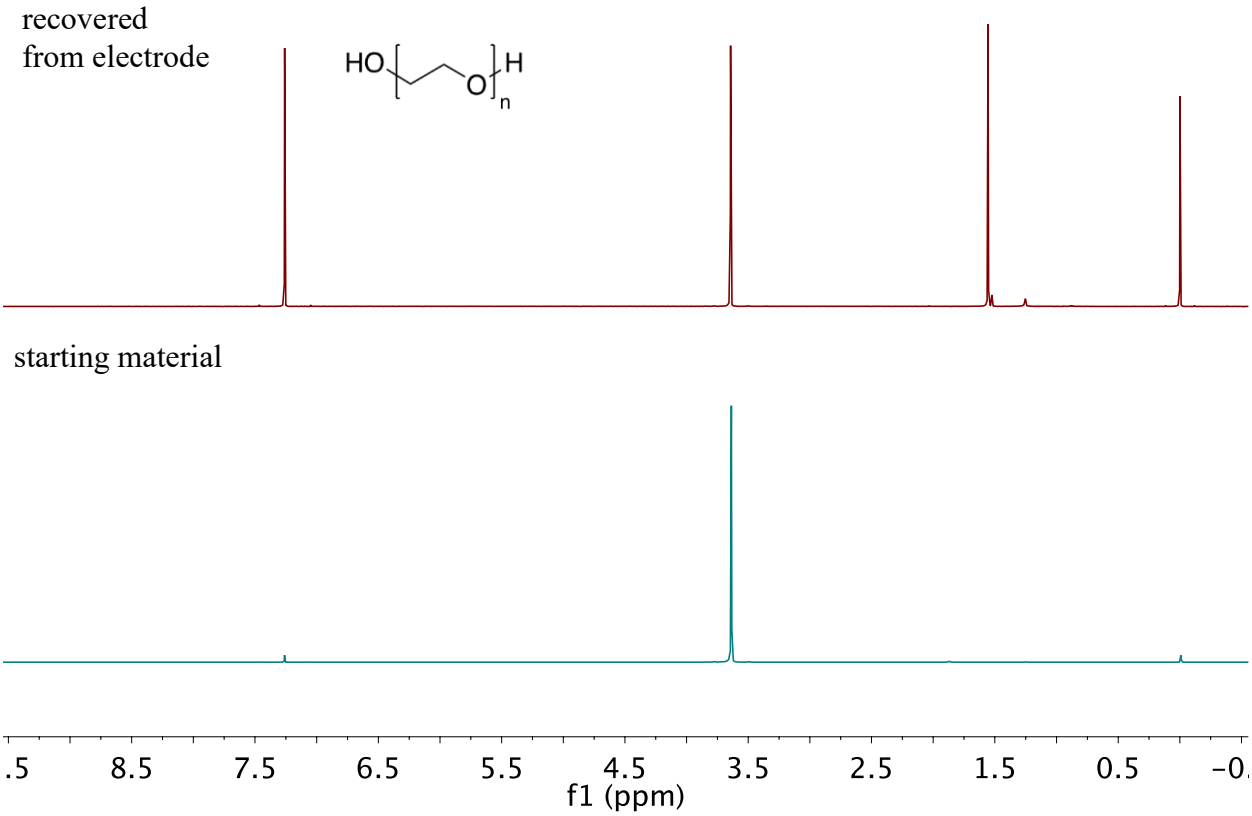

Figure S.18 ^{1}H NMR of commercial polyethylene glycol (**6**) in $CDCl_3$ (bottom), compared with rinse of electrode after 65 minutes of chronoamperometry, also in $CDCl_3$ (top).

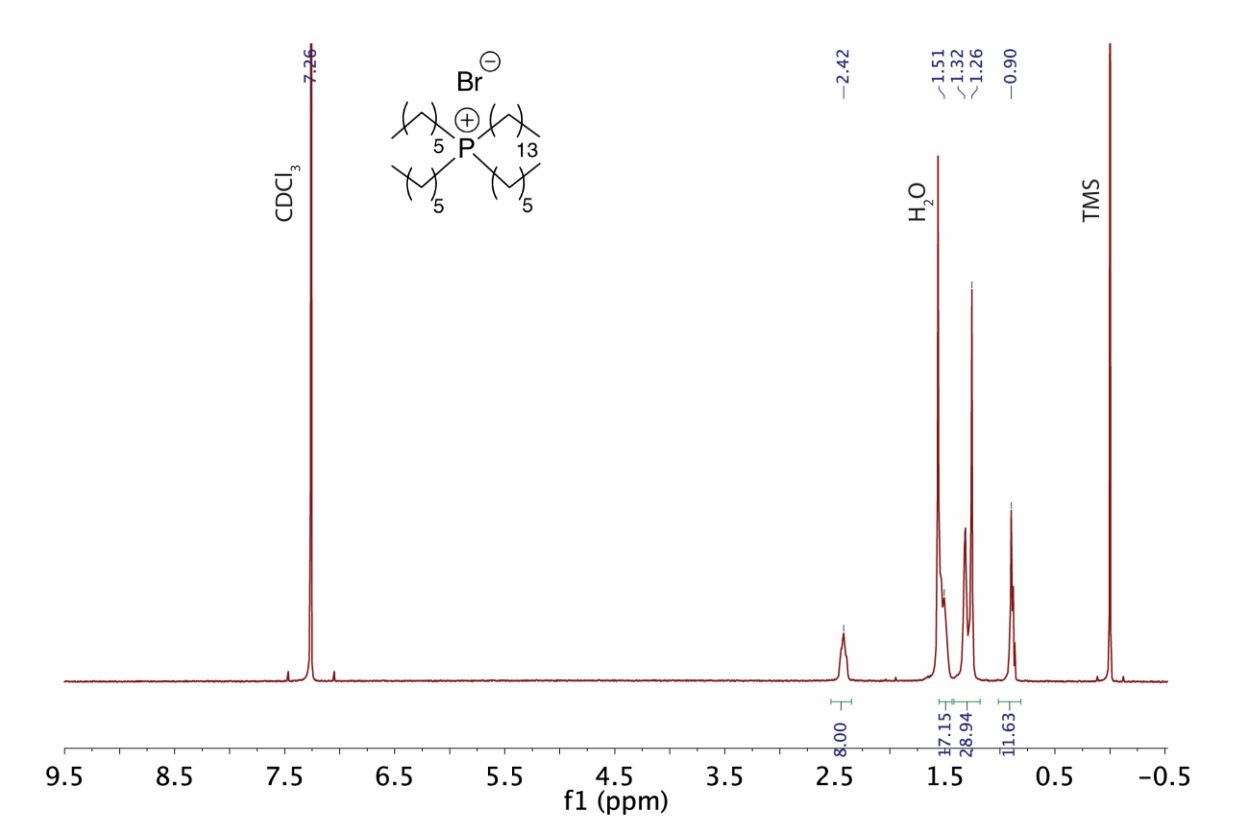

Figure S19. [1]H NMR of trihexyltetradecylphosphonium bromide (**7**), rinsed from electrode after 65 minutes of chronoamperometry.

The CA experiment was conducted as described in the Experimental Methods, except with an increase in the loading. A 50 mg sample of trihexyltetradecylphosphonium bromide (**7**) was dissolved in 1 mL iPrOH, and 100 µL of this solution was dropcast onto the oxide-derived Cu surface. 50 µL of Nafion solution was dissolved in 1 mL of iPrOH, and 100 µL of the Nafion solution was then dropcast onto the functionalized Cu surface.

^{1}H NMR (500 MHz, $CDCl_3$, ppm): δ 2.42 (m, 8H), 1.51-1.26 (m, 48H), 0.90 (m, 12H).

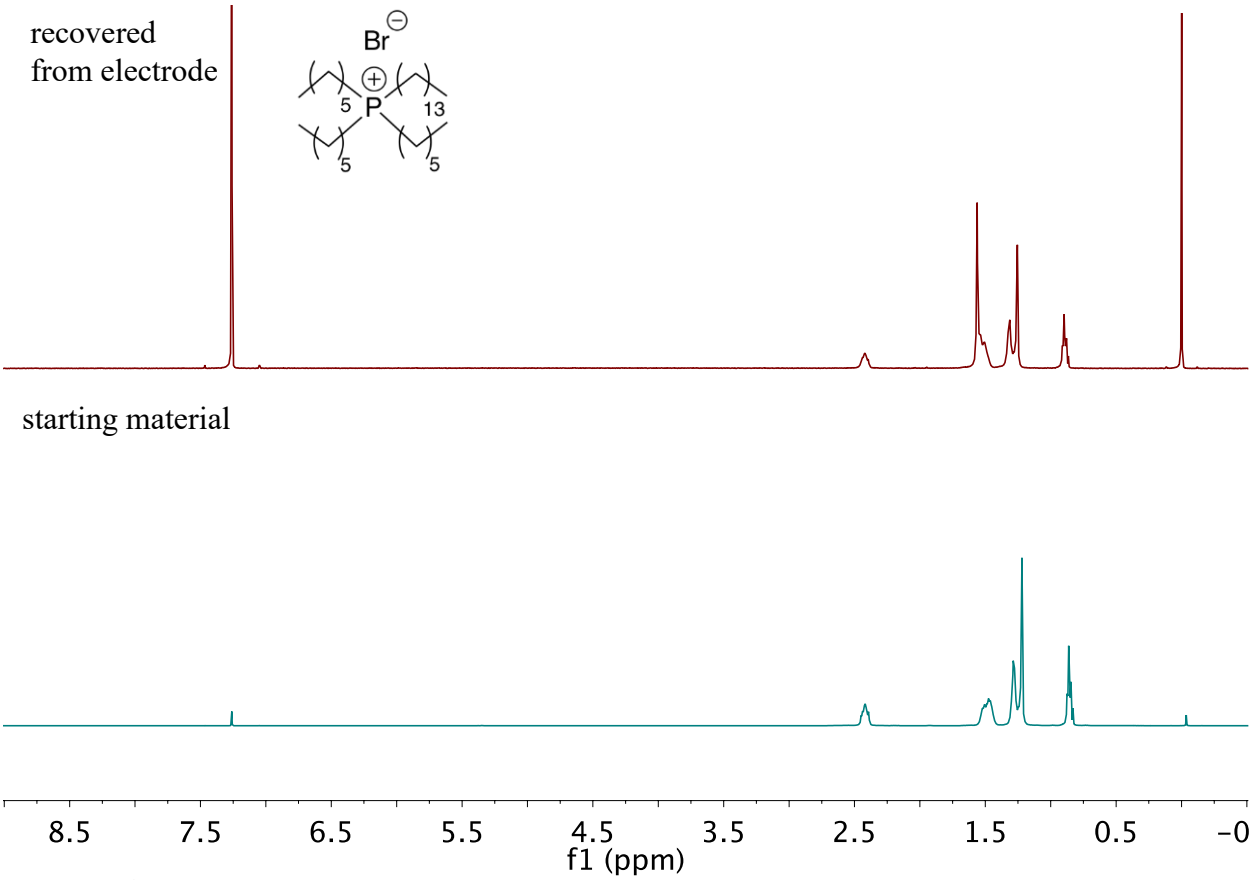

Fig. S20. ^{1}H NMR of commercial trihexyltetradecylphosphonium bromide (**7**) in $CDCl_3$ (bottom), compared with rinse of electrode after 65 minutes of chronoamperometry, also in $CDCl_3$ (top).

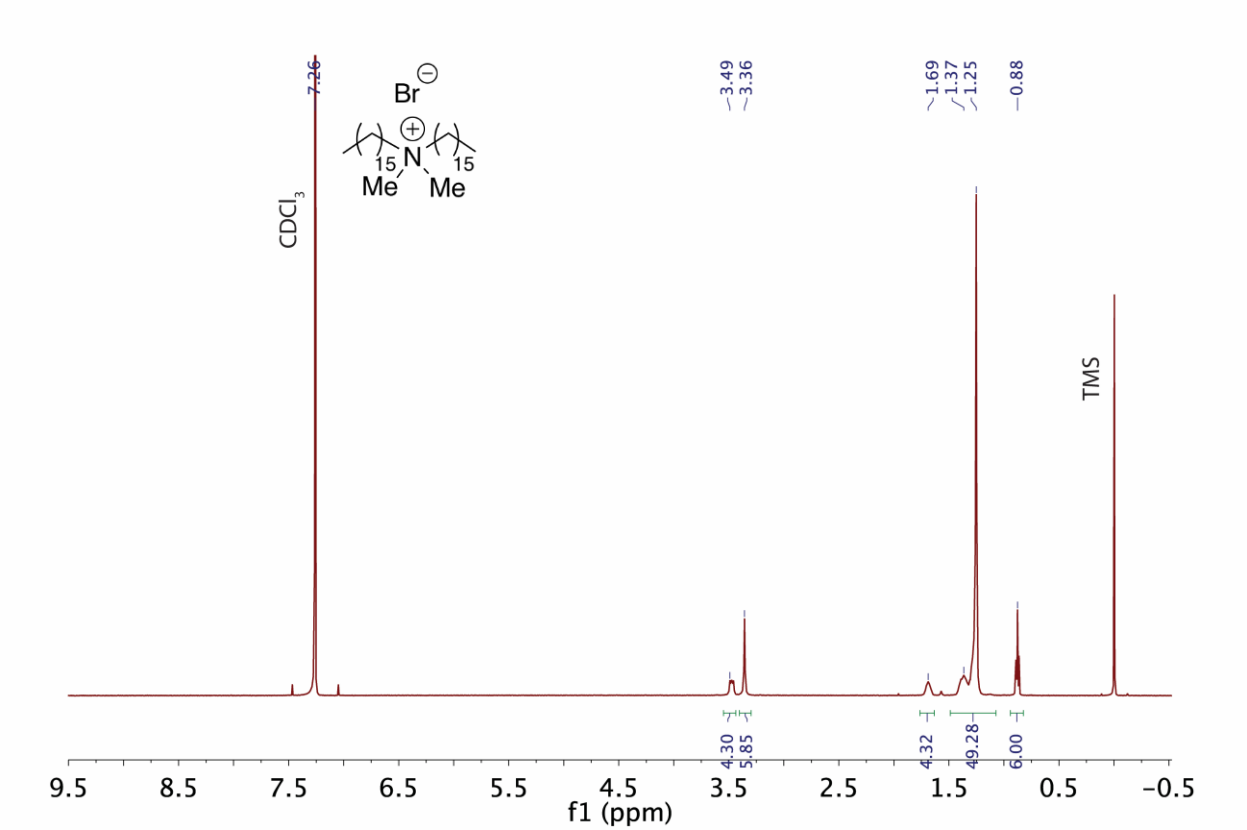

Figure S21. [1]H NMR of dihexadecyldimethylammonium bromide (**8**), rinsed from electrode after 65 minutes of chronoamperometry.

The CA experiment was conducted as described in the Experimental Methods, except with an increase in the loading. A 50 mg sample of dihexadecyldimethylammonium bromide (**8**) was dissolved in 1 mL iPrOH, and 100 µL of this solution was dropcast onto the oxide-derived Cu surface. 50 µL of Nafion solution was dissolved in 1 mL of iPrOH, and 100 µL of the Nafion solution was then dropcast onto the functionalized Cu surface.

^{1}H NMR (500 MHz, $CDCl_3$, ppm): δ 3.49 (m, 4H), 3.36 (s, 6H), 1.69 (m, 4H), 1.37-1.25 (m, 52H), 0.88 (t, J = 7.09, 6H).

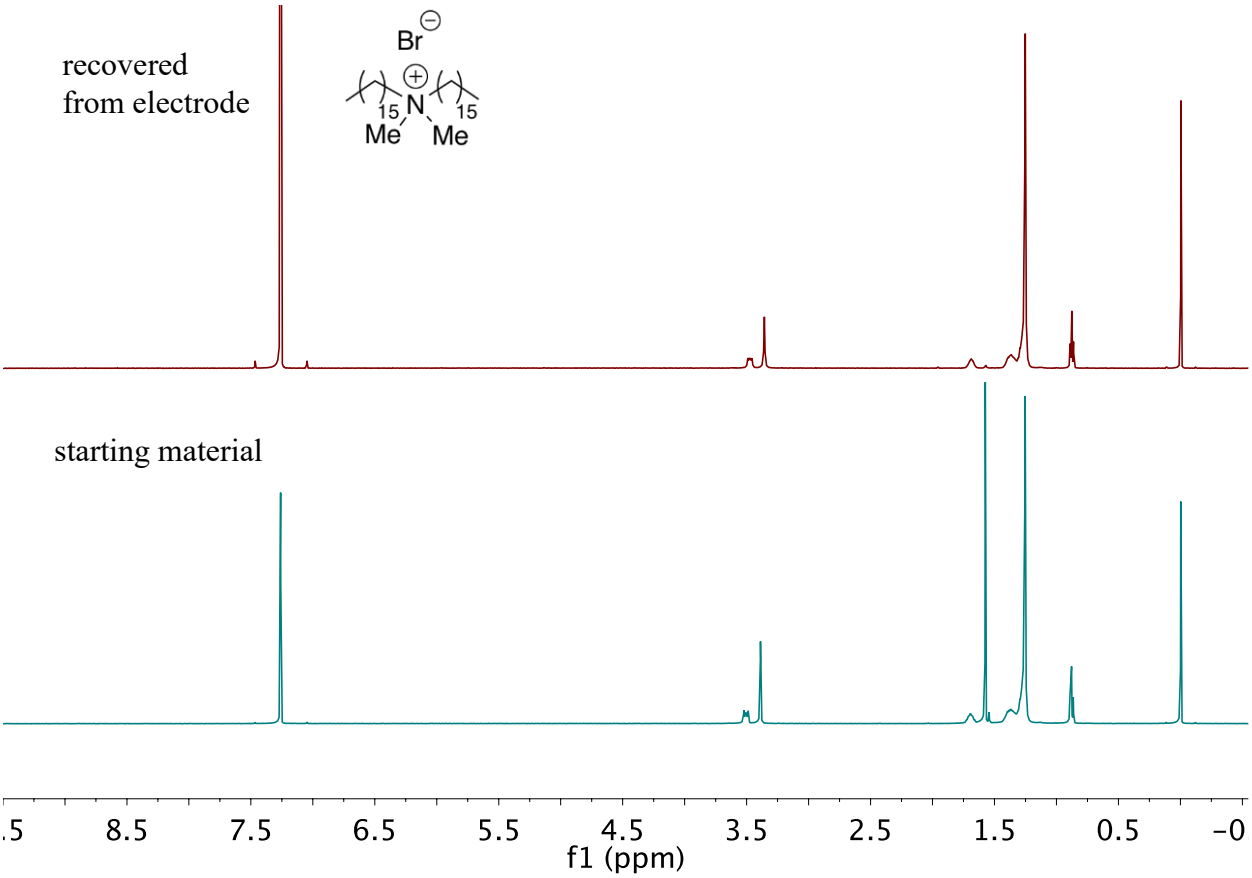

Figure S22. ^{1}H NMR of commercial dihexadecyldimethylammonium bromide (**8**) in $CDCl_3$ (bottom), compared with rinse of electrode after 65 minutes of chronoamperometry, also in $CDCl_3$ (top).

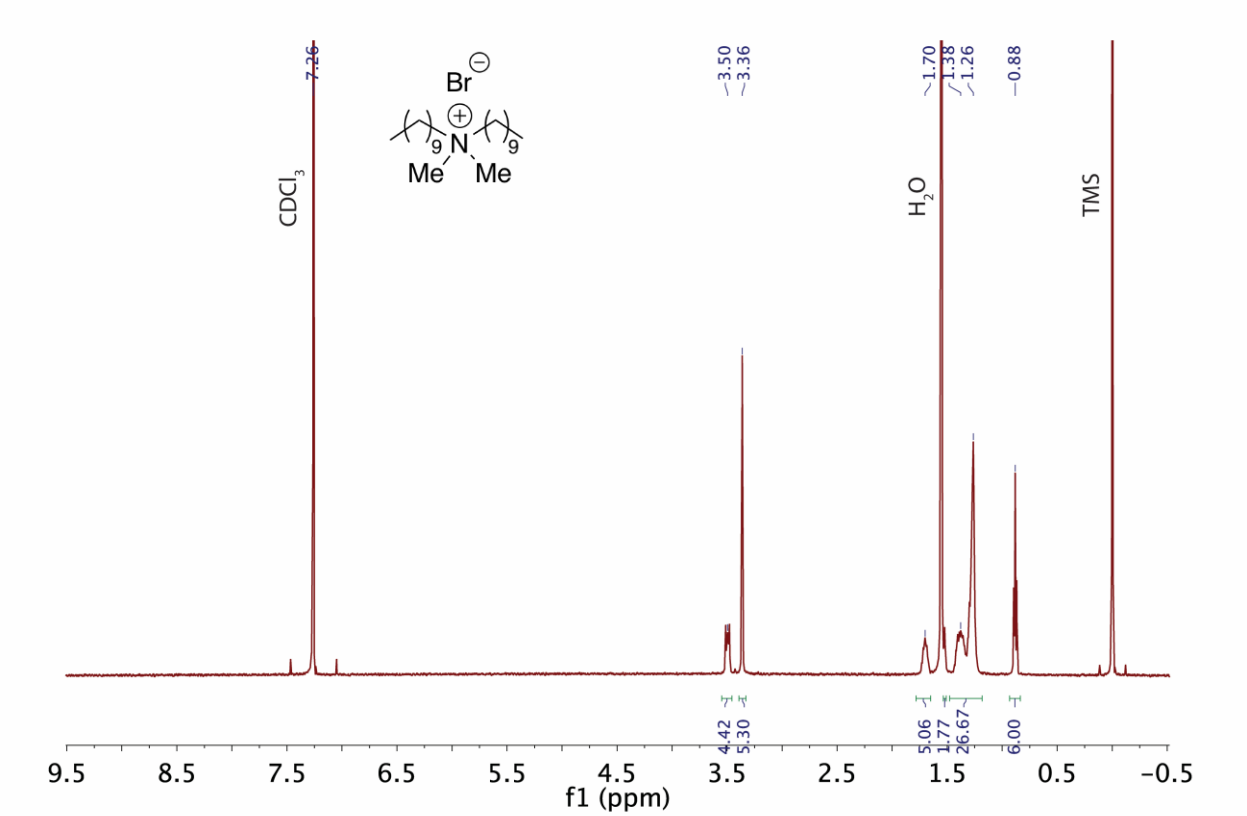

Figure S23. ^{1}H NMR of didecyldimethylammonium bromide (**9**), rinsed from electrode after 65 minutes of chronoamperometry.

The CA experiment was conducted as described in the Experimental Methods, except with an increase in the loading. A 20 mg sample of didecyldimethylammonium bromide (**9**) was dissolved in 1 mL iPrOH, and 100 µL of this solution was dropcast onto the oxide-derived Cu surface. 20 µL of Nafion solution was dissolved in 1 mL of iPrOH, and 100 µL of the Nafion solution was then dropcast onto the functionalized Cu surface.

^{1}H NMR (500 MHz, $CDCl_3$, ppm): δ 3.50 (m, 4H), 3.36 (s, 6H), 1.70 (m, 4H), 1.38-1.26 (m, 28H), 0.88 (t, J = 6.75, 6H).

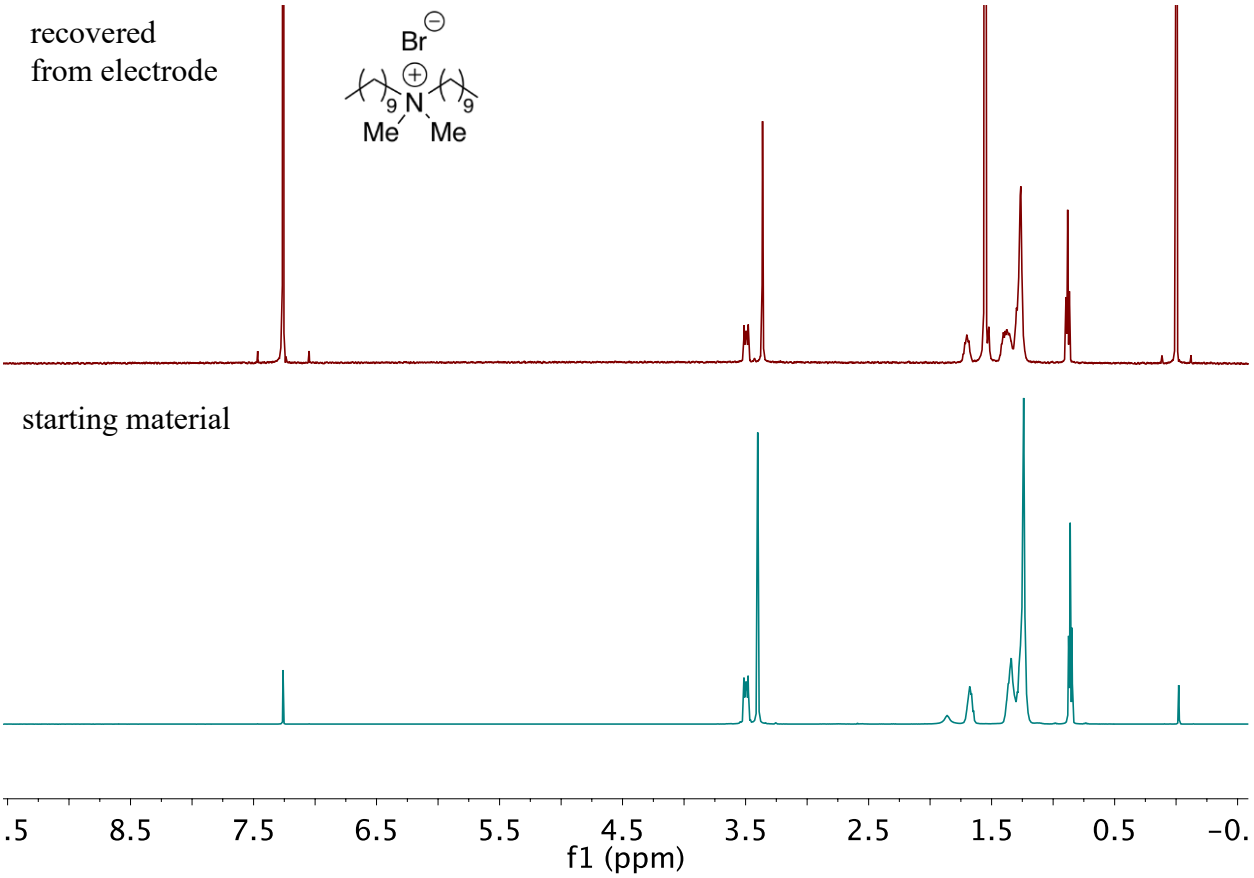

Figure S.24 ^{1}H NMR of commercial didecyldimethylammonium bromide (**9**) in $CDCl_3$ (bottom), compared with rinse of electrode after 65 minutes of chronoamperometry, also in $CDCl_3$ (top).

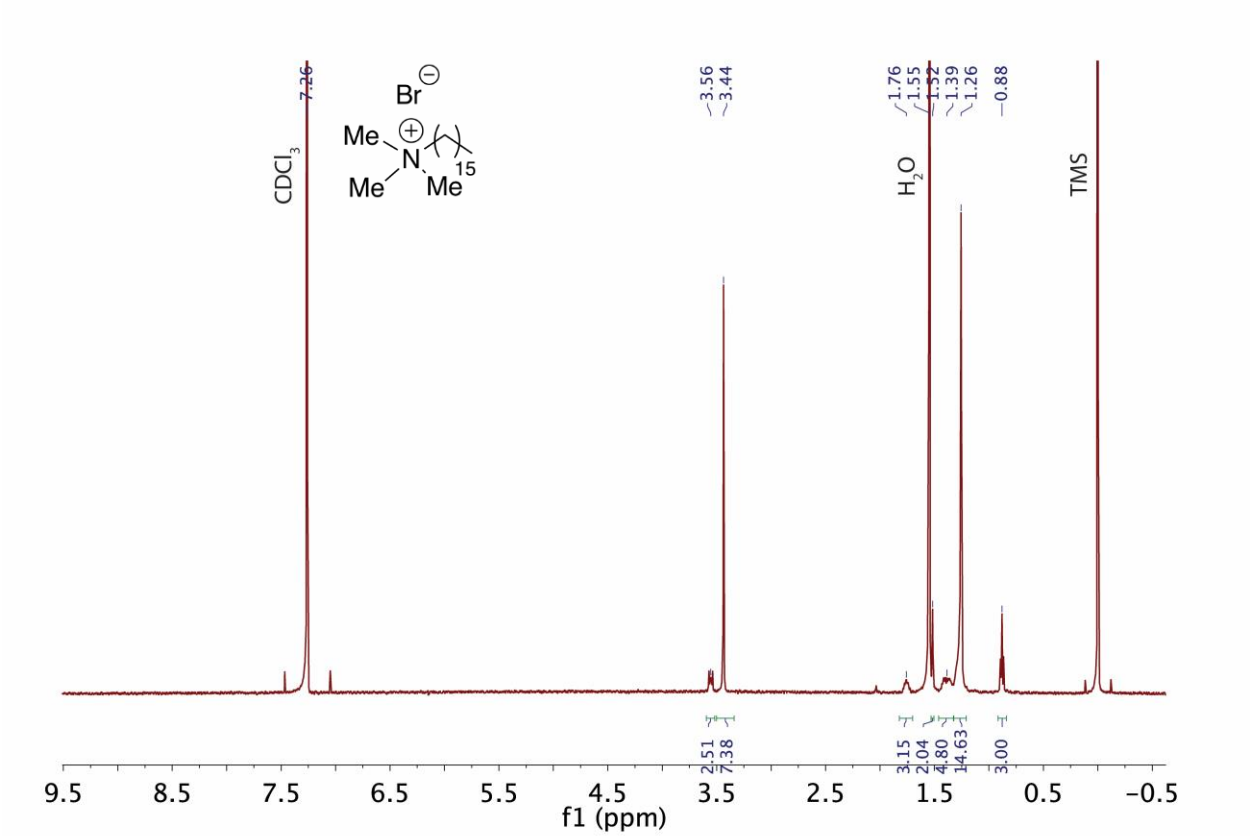

Figure S25. [1]H NMR of cetyltrimethylammonium bromide (**10**), rinsed from electrode after 65 minutes of chronoamperometry.

The CA experiment was conducted as described in the Experimental Methods, except with an increase in the loading. A 20 mg sample of cetyltrimethylammonium bromide (**10**) was dissolved in 1 mL iPrOH, and 100 µL of this solution was dropcast onto the oxide-derived Cu surface. 20 µL of Nafion solution was dissolved in 1 mL of iPrOH, and 100 µL of the Nafion solution was then dropcast onto the functionalized Cu surface.

^{1}H NMR (500 MHz, $CDCl_3$, ppm): δ 3.56 (m, 2H), 3.44 (s, 9H), 1.76-1.26 (m, 28H), 0.88 (t, J = 6.70, 3H).

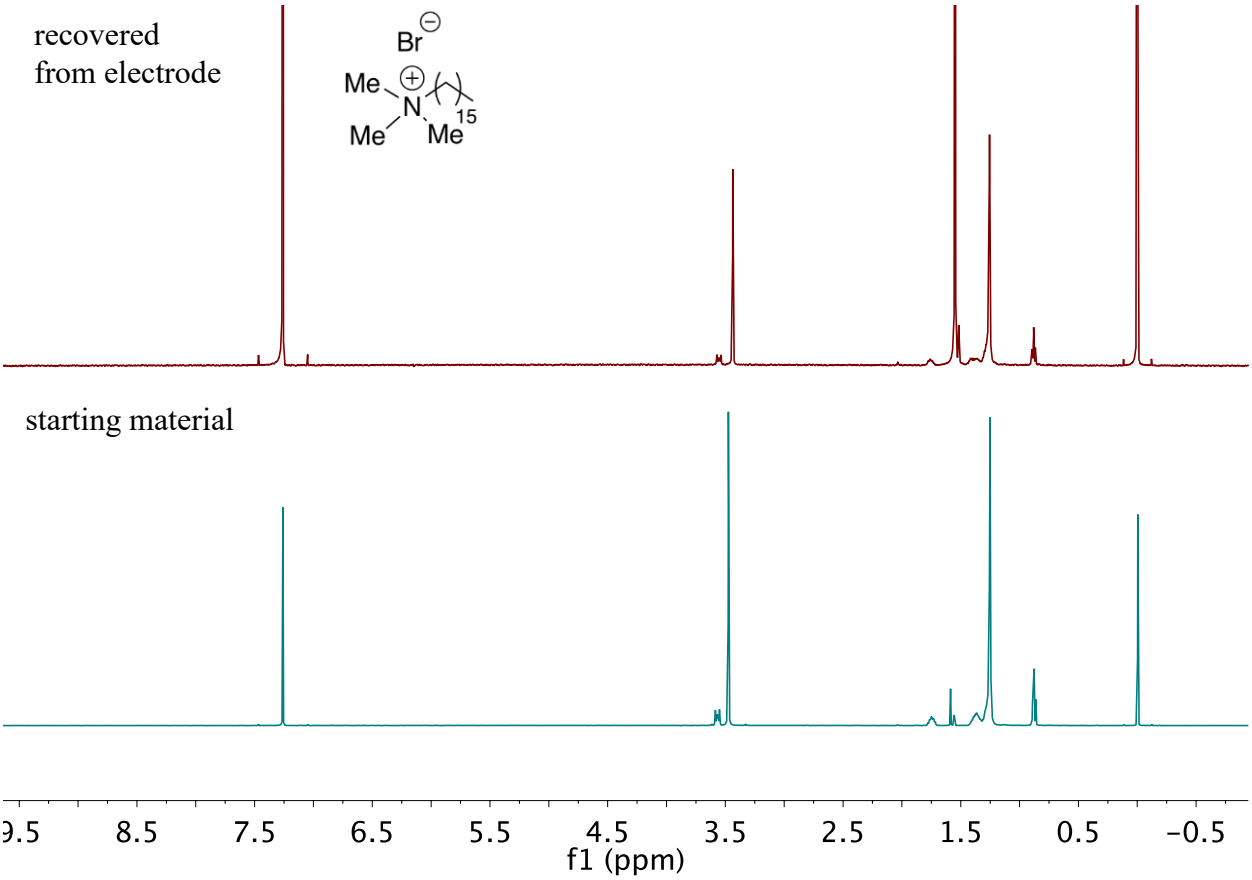

Fig. S26. ^{1}H NMR of commercial cetyltrimethylammonium bromide (**10**) in $CDCl_3$ (bottom), compared with rinse of electrode after 65 minutes of chronoamperometry, also in $CDCl_3$ (top).

SH. Partial current densities

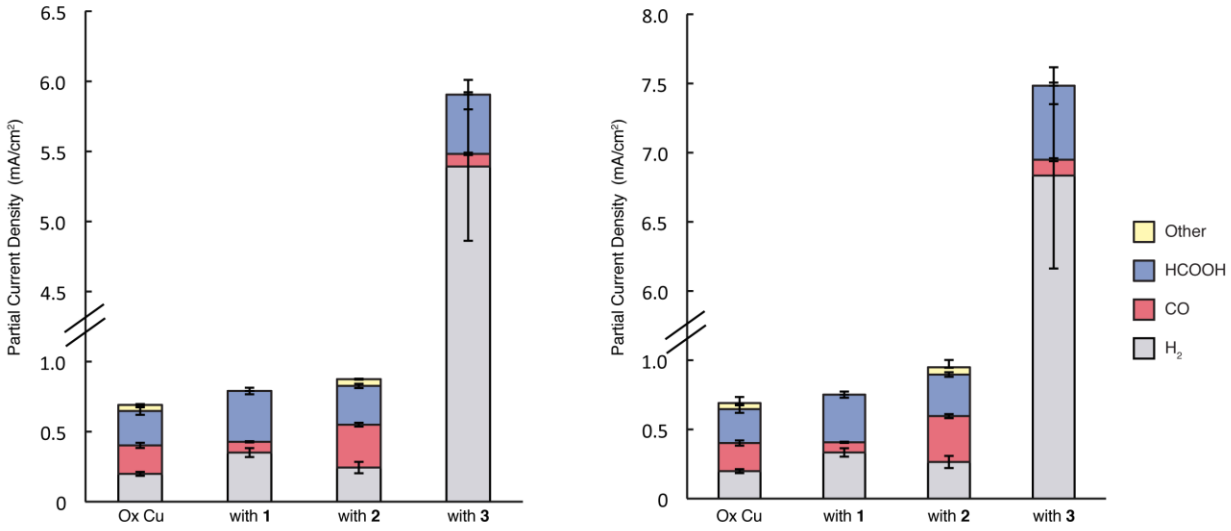

Fig. S27. Partial current densities for H_2, CO and formic acid as determined by GC and HPLC (left) and normalized by double layer capacitance (right). The double layer capacitance of the modified surface after chronoamperometry was compared to that of unmodified oxide-derived copper, and the ratio of these values was used to normalize the partial current densities. Error bars illustrate the standard error of the mean.

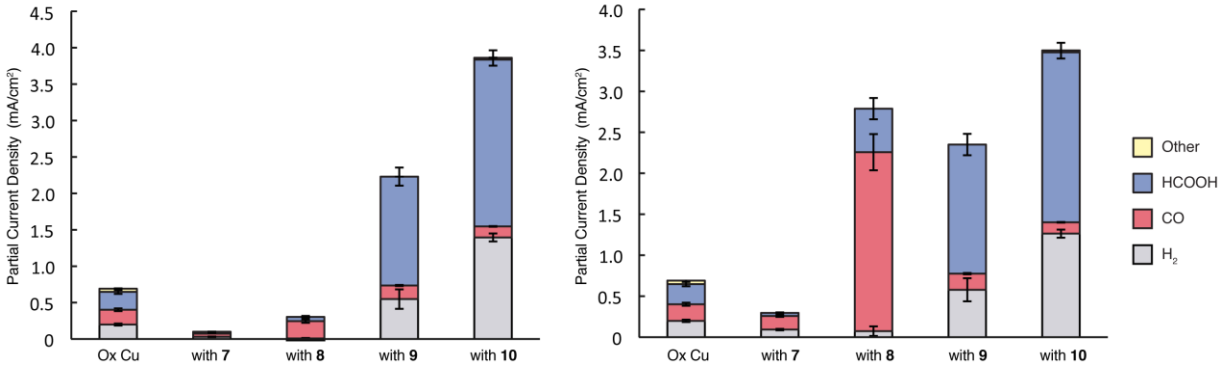

Fig. S28. Partial current densities for H_2, CO and formic acid as determined by GC and HPLC (left) and normalized by double layer capacitance (right). The double layer capacitance of the modified surface after chronoamperometry was compared to that of unmodified oxide-derived copper, and the ratio of these values was used to normalize the partial current densities. Error bars illustrate the standard error of the mean.

SI. Contact angle and summarized product distribution data

Table S5. Contact angle measurements, CO2R selectivity and total current for modified Cu surfaces. Modifiers are listed in order of increasing hydrophobicity. Error values are derived from standard error of the mean.

Sample	Contact Angle (˚)	H_2 (%)	CO (%)	Formic acid (%)	Other (%)	Total FE (%)	Total current (mA/cm^2)
*Cetyltrimethyl ammonium bromide (**10**)*	**5.4**±0.9	**34**±1	**3.64**± 0.05	**56**±2	**0.08** ±0.05	**93**±1	**4.17**±0.15
*Polyvinyl pyrrolidone (**1**)*	**11**±2	**43**±1	**10**±1	**45**±2	**0**	**98**±1	**0.81**±0.05
*Didecyldimethyl ammonium bromide (**9**)*	**13**±4	**21**±3	**8**±1	**62**±3	**0**	**91**±2	**2.45**±0.29
*Polyethylene glycol (**6**)*	**14**±3	**44**±6	**16**±3	**38**±3	**0**	**98**±2	**0.70**±0.08
Ox Cu	**27**±4	**28**±2	**28**±2	**34**±3	**6.0** ±0.6	**96**±2	**0.73**±0.05
*Polyvinyl alcohol (**5**)*	**40**±10	**71**±2	**15.1**± 0.6	**17**±1	**0**	**103**±1	**0.54**±0.06
*Dihexadecyl dimethylammo-nium bromide (**8**)*	**48**±3	**3**±2	**76**±5	**18**±4	**0**	**97**±1	**0.31** ±0.03
*Trihexyltetra decylphospho-nium bromide (**7**)*	**48**±4	**27**±2	**49**±3	**11**±2	**0**	**87**±4	**0.115** ±0.003
*Polyallylamine (**3**)*	**54**±4	**97**±2	**1.63** ±0.04	**8**±1	**0**	**106.4** ±0.4	**5.6** ±0.6
*Tetrahexadecyl ammonium bromide (**2**)*	**65**±5	**27**±3	**33.8** ±0.9	**30.5** ±0.4	**5.4** ±0.6	**96** ±2	**0.91** ±0.05
*Polystyrene (**4**)*	**97**±3	**44.6** ±0.6	**19**±2	**23.5**± 0.8	**3.5** ±0.7	**91**±2	**0.80**±0.13

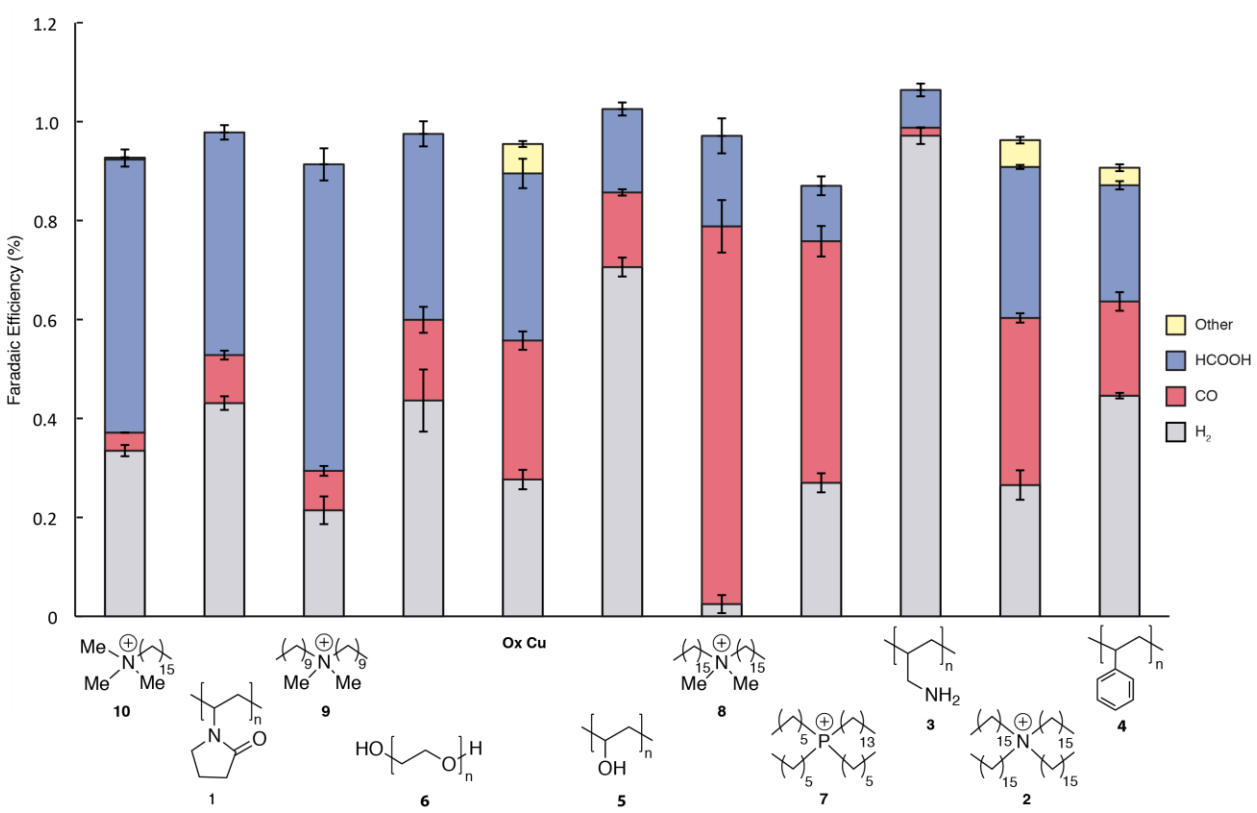

Figure S29. Faradaic efficiencies for modified Cu surfaces, from most hydrophilic (left) to hydrophobic (right). Graphical representation of the data presented in **Table S5**.

Table S6. Contact angle measurements, CO2R partial current densities and total current for modified Cu surfaces. Modifiers are listed in order of increasing hydrophobicity. Error values are derived from standard error of the mean.

Sample	Contact Angle (˚)	H_2 (mA/cm²)	CO (mA/cm²)	formic acid (mA/cm²)	Other (mA/cm²)	Total current (mA/cm²)
*Cetyltrimethyl ammonium bromide (**10**)*	**5.4**±0.9	**1.39**±0.05	**0.151**±0.004	**2.3**±0.1	**0.003**±0.002	**4.17**±0.15
*Polyvinyl pyrrolidone (**1**)*	**11**±2	**0.35**±0.03	**0.077**±0.004	**0.36**±0.02	**0**	**0.81**±0.05
*Didecyldimethyl ammonium bromide (**9**)*	**13**±4	**0.5**±0.1	**0.187**±0.008	**1.5**±0.1	**0**	**2.45**±0.29
*Polyethylene glycol (**6**)*	**14**±3	**0.32**±0.08	**0.108**±0.005	**0.26**±0.02	**0**	**0.70**±0.08
Ox Cu	**27**±4	**0.20**±0.01	**0.20**±0.02	**0.25**±0.03	**0.043**±0.005	**0.73**±0.05
*Polyvinyl alcohol (**5**)*	**40**±10	**0.38**±0.03	**0.080**±0.006	**0.09**±0.01	**0**	**0.54**±0.06
*Dihexadecyldi-methylammonium bromide (**8**)*	**48**±3	**0.008**±0.006	**0.24**±0.02	**0.06**±0.01	**0**	**0.31**±0.03
*Trihexyltetradecyl phosphonium bromide (**7**)*	**48**±4	**0.031**±0.003	**0.056**±0.003	**0.013**±0.002	**0**	**0.115**±0.003
*Polyallylamine (**3**)*	**54**±4	**5.4**±0.5	**0.090**±0.008	**0.4**±0.1	**0**	**5.6**±0.6
*Tetrahexadecyl ammonium bromide (**2**)*	**65**±5	**0.24**±0.04	**0.31**±0.01	**0.28**±0.02	**0.048**±0.004	**0.91**±0.05
*Polystyrene (**4**)*	**97**±3	**0.36**±0.05	**0.15**±0.01	**0.19**±0.03	**0.029**±0.009	**0.80**±0.13

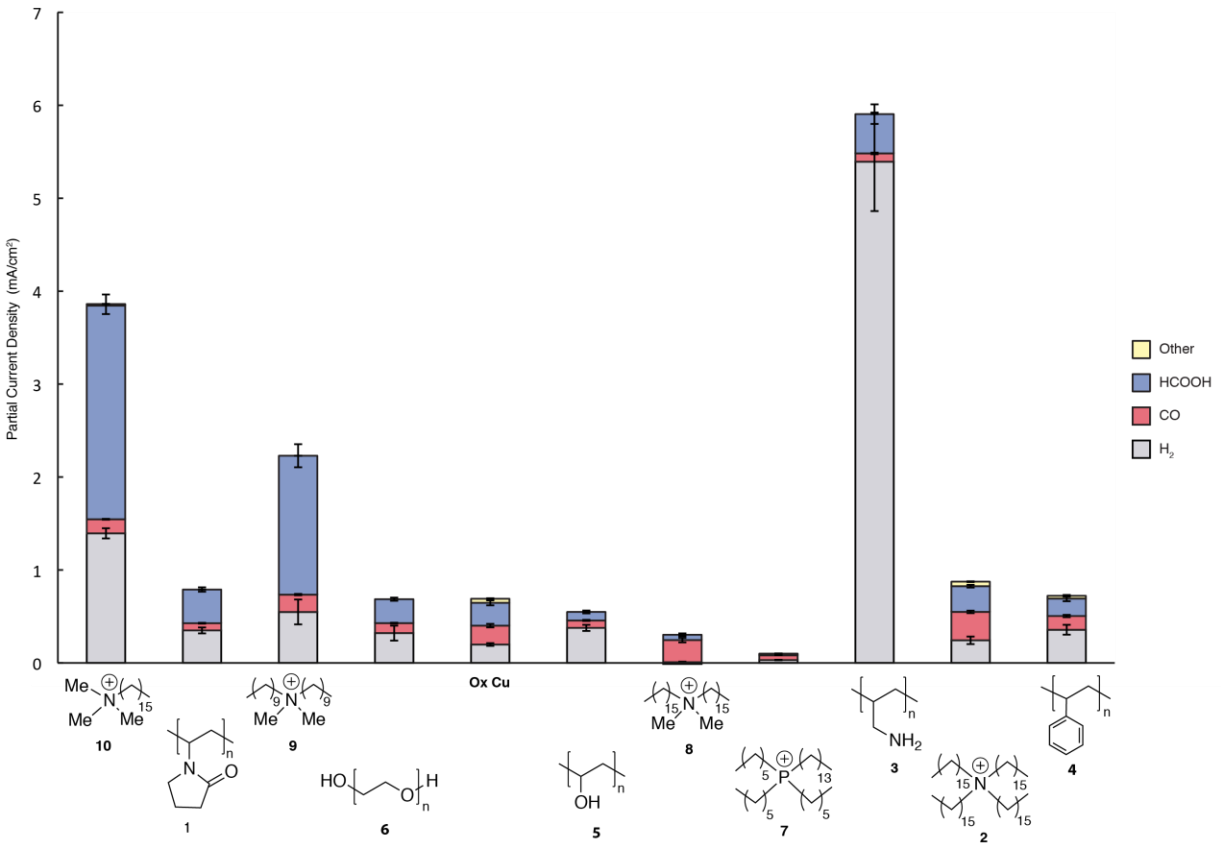

Figure S30. Partial current densities for modified Cu surfaces, from most hydrophilic (left) to hydrophobic (right). Graphical representation of the data presented in **Table S6**.

SJ. Relationship between Faradaic efficiency for CO, H_2 and the contact angle

Fig. 4b in the main text illustrates the relationship between the Faradaic efficiency for formic acid and the contact angle of the Cu surfaces in the text, including **Ox Cu** and with modifiers **1** – **10**. **Fig. S31** and **Fig. S32** below illustrate this relationship for CO and H_2.

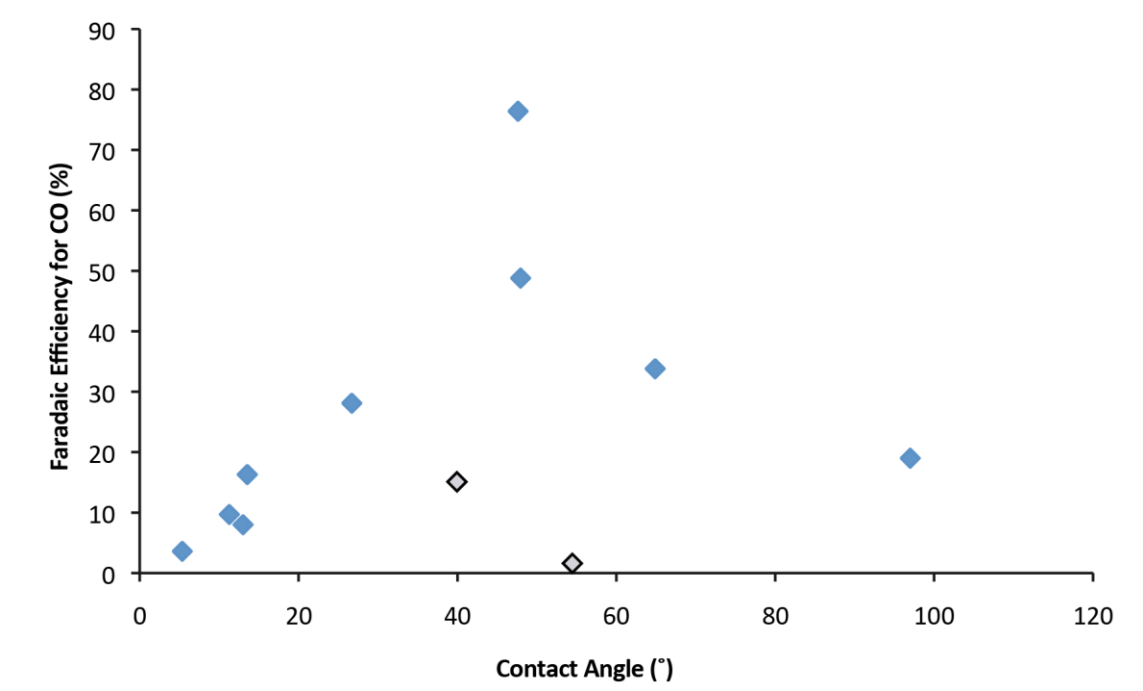

Figure S31. Relationship between Faradaic efficiency for CO and the contact angle of water on modified Cu surfaces. Data points in gray are protic species polyallylamine (**3**) and polyvinyl alcohol (**5**).

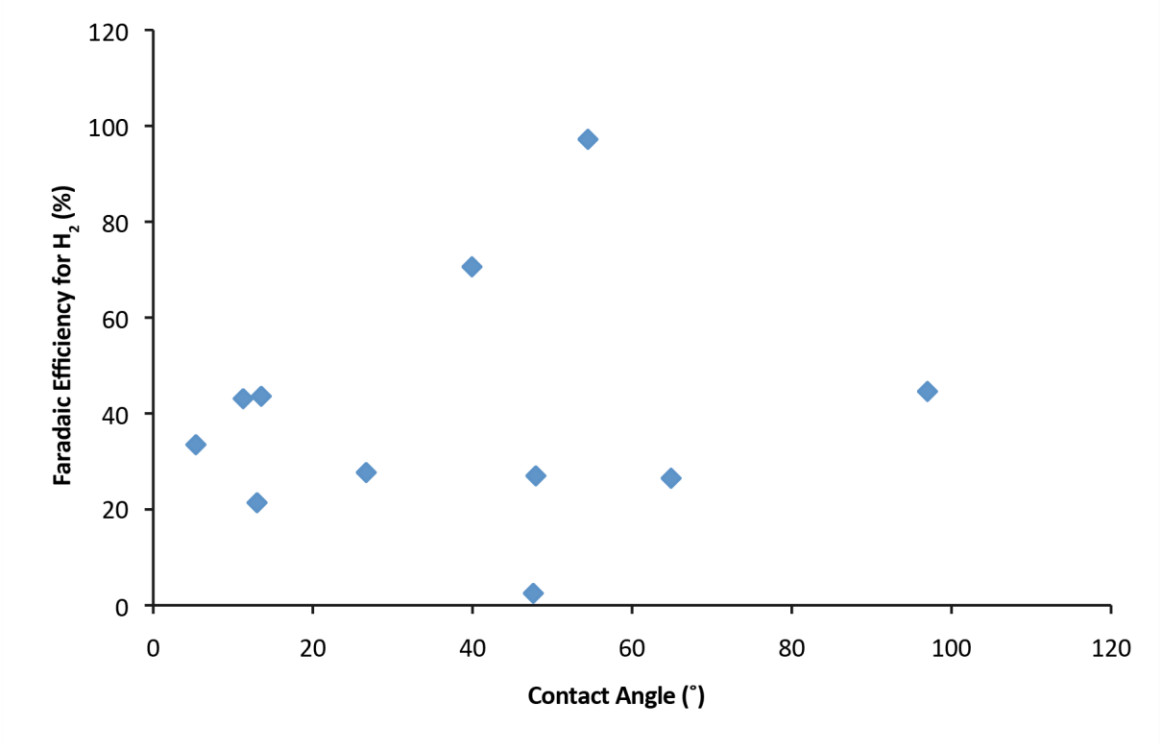

Figure S32. Relationship between Faradaic efficiency for H_2 and the contact angle of water on modified Cu surfaces. The selectivity for H_2 does not show a clear relationship with the contact angle of the modified surface. This may be due to the fact that the selectivity illustrates the amount of product formed relative to the amounts of the other products, which may convolute different trends. Examination of the amount of product formed (the partial current density), instead of the relative amount of product, indicates that the amount of H_2 formed decreases as the hydrophobicity increases, with **2** and **4** as outliers at 65˚ and 97˚, respectively (see **Fig. S33** below).

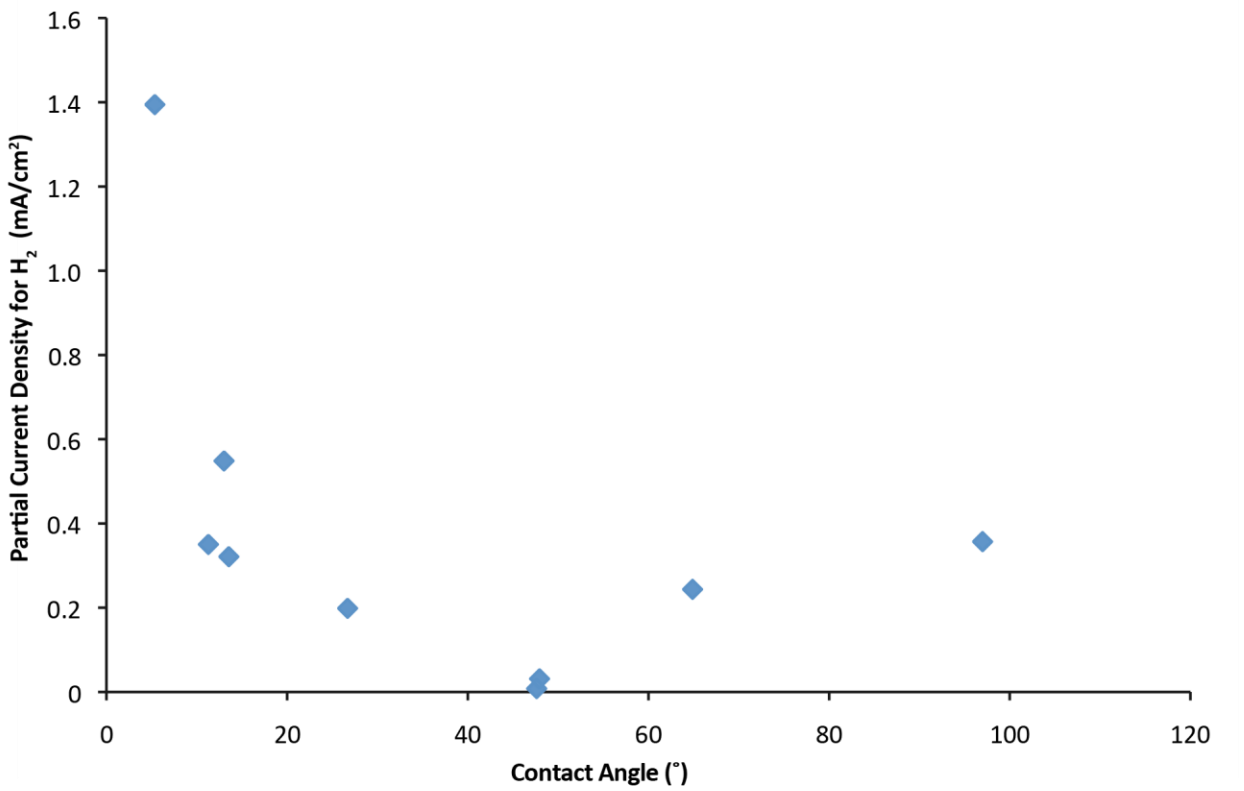

Figure S33. Relationship between partial current density for H_2 and the contact angle of water on modified Cu surfaces. Polyallylamine (**3**) and polyvinyl alcohol (**5**) are not included due to the enhanced activity for H_2 observed with these protic species.

SK. Relationship between formation of H_2, CO and formic acid

In order to better understand the relationship between the formation of these three products, the partial current densities towards these products generated with Ox Cu and modified surfaces (excluding protic modifiers **3** and **5**) were plotted against each other. Fig. S34 suggests that the formation of formic acid and H_2 may be related, while no such relationship emerges from Fig. S35 and Fig. S36.

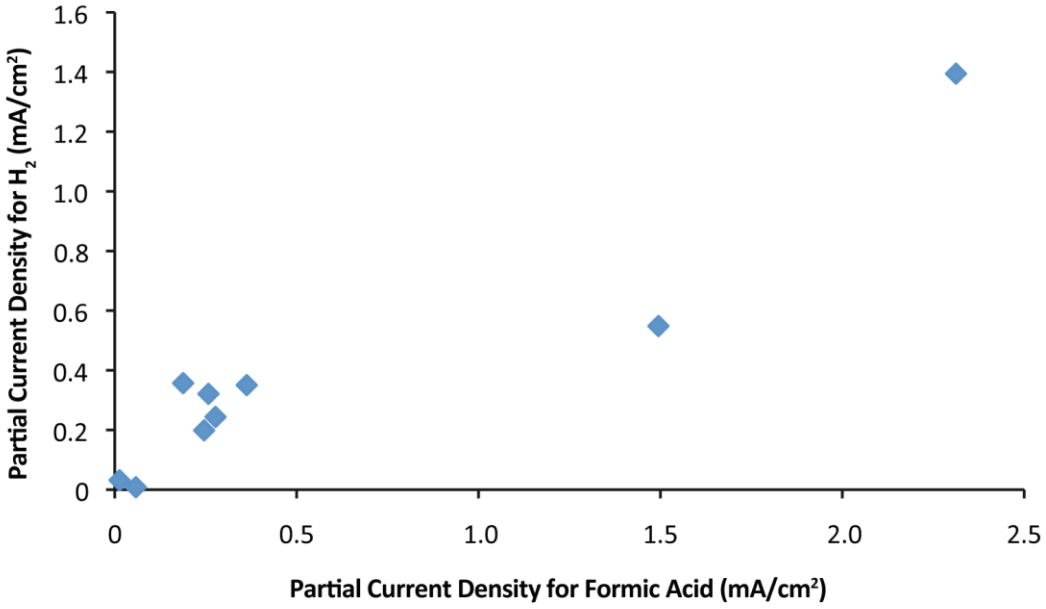

Figure S34. Plot of partial current of formic acid vs. partial current of H_2 from Ox Cu and modified surfaces.

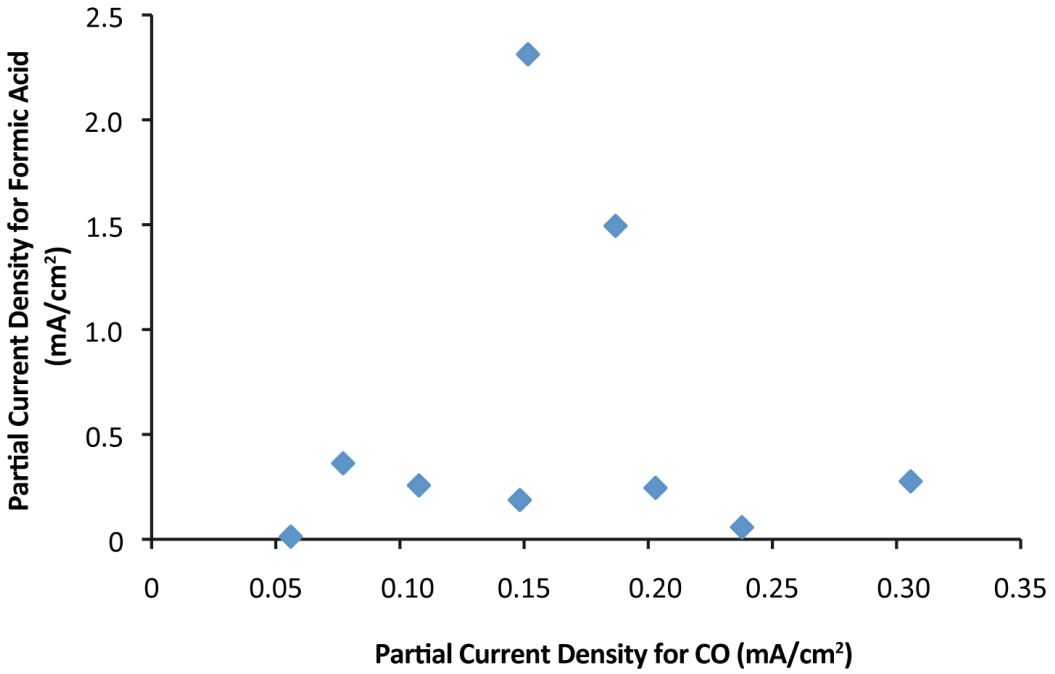

Figure S35. Plot of partial current of CO vs. partial current of formic acid from Ox Cu and modified surfaces.

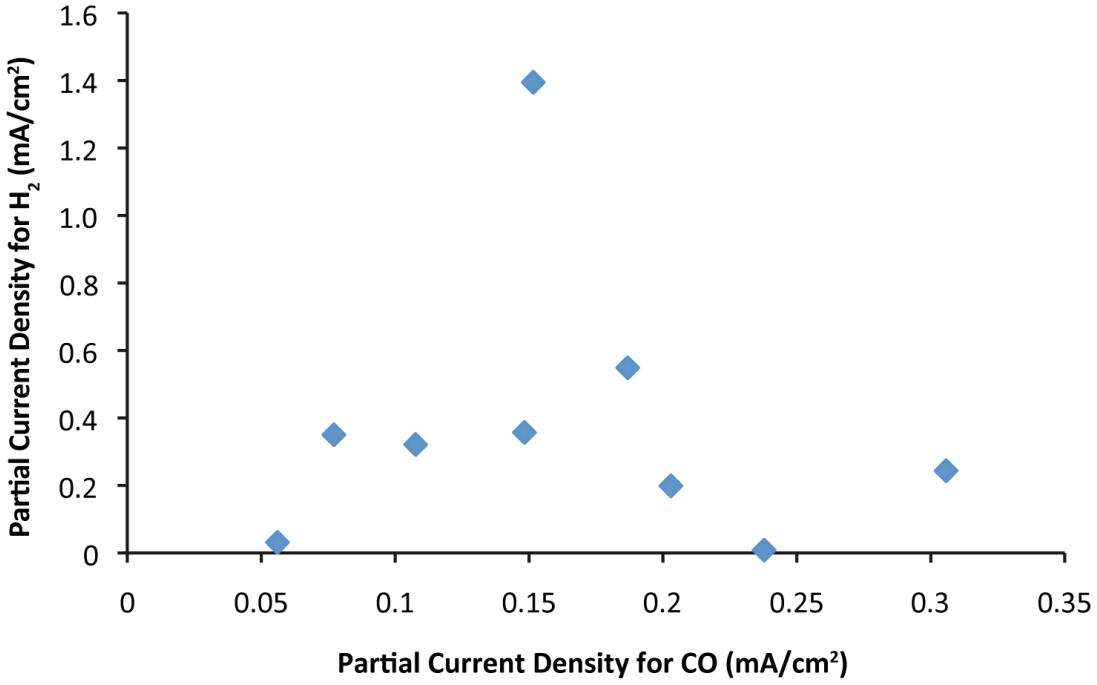

Figure S36. Plot of partial current of CO vs. partial current of H_2 from Ox Cu and modified surfaces.

SL. Tables of Faradaic efficiency data

Tables include standard error of the mean (SEM) and standard deviation (STD). The STD illustrates the spread of the distribution of the data, while the SEM provides a measure of how the sample mean relates to the population mean, or the typical uncertainty for a measurement. The discussion of the main manuscript focuses upon the trends observed between various modifiers, rather than the observed quantities, and so SEM is employed in the text and figures of the main manuscript, while both values are reported below.

Table S7. Data for Figure 1

A	**Ox Cu**	**H_2**	**CO**	**Formic Acid**	**Other**	**Total FE**	**Total Current (mA/cm^2)**
	Average	**28%**	**28%**	**34%**	**6.0%**	**96%**	**0.73**
	SEM	**2%**	**2%**	**3%**	**0.6%**	**2%**	**0.05**
	STD	**4%**	**4%**	**7%**	**1%**	**5%**	**0.12**
	Trial 1	27%	24%	36%	6.9%	95%	0.86
	Trial 2	23%	29%	44%	7.6%	103%	0.66
	Trial 3	24%	34%	27%	5.3%	91%	0.79
	Trial 4	29%	24%	33%	5.6%	92%	0.77
	Trial 5	34%	29%	29%	4.4%	97%	0.55

B	Polyvinylpyrrolidone (**1**)	**H_2**	**CO**	**Formic Acid**	**Other**	**Total FE**	**Total Current (mA/cm^2)**
	Average	**43%**	**10%**	**45%**	**0%**	**98%**	**0.81**
	SEM	**1%**	**1%**	**2%**	**0%**	**1%**	**0.05**
	STD	**3%**	**2%**	**3%**	**0%**	**2%**	**0.12**
	Trial 1	46%	9%	42%	0%	97%	0.79
	Trial 2	38%	13%	51%	0%	102%	0.71
	Trial 3	45%	8%	45%	0%	98%	1.01
	Trial 4	44%	9%	44%	0%	96%	0.82
	Trial 5	42%	10%	44%	0%	96%	0.71

C	Tetrahexadecylammonium bromide (**2**)	**H_2**	**CO**	**Formic Acid**	**Other**	**Total FE**	**Total Current (mA/cm^2)**
	Average	**27%**	**33.8%**	**30.5%**	**5.4%**	**96%**	**0.91**
	SEM	**3%**	**0.9%**	**0.4%**	**0.6%**	**2%**	**0.05**
	STD	**5%**	**2%**	**0.7%**	**1%**	**3%**	**0.08**
	Trial 1	26%	32.5%	29.7%	6.0%	94%	0.88
	Trial 2	32%	33.2%	30.7%	4.1%	100%	1.00
	Trial 3	22%	35.6%	31.1%	6.1%	95%	0.84

D	Polyallylamine (**3**)	**H_2**	**CO**	**Formic Acid**	**Other**	**Total FE**	**Total Current (mA/cm^2)**
	Average	**97%**	**1.63%**	**8%**	**0%**	**106.4%**	**5.6**
	SEM	**2%**	**0.04%**	**1%**	**0%**	**0.4%**	**0.6**
	STD	**3%**	**0.1%**	**2%**	**0%**	**0.7%**	**1.0**

Trial 1	100%	1.68%	5%	0%	107.0%	4.4
Trial 2	97%	1.54%	8%	0%	106.5%	6.3
Trial 3	94%	1.66%	10%	0%	105.6%	6.0

Table S8. Data for Table 1

Ox Cu, polyvinylpyrrolidone (**1**) and polyallylamine (**3**) may be found in **Table S6.**

A	*Polystyrene (**4**)*	**H_2**	**CO**	**Formic Acid**	**Other**	**Total FE**	**Total Current (mA/cm^2)**
	Average	**44.6%**	**19%**	**23.5%**	**3.5%**	**91%**	**0.80**
	SEM	**0.6%**	**2%**	**0.8%**	**0.7%**	**2%**	**0.13**
	STD	**1%**	**3%**	**1%**	**1.2%**	**4%**	**0.2**
	Trial 1	43.8%	18%	24.2%	3.0%	89%	0.95
	Trial 2	44.3%	17%	21.8%	4.9%	88%	0.91
	Trial 3	45.7%	23%	24.5%	2.7%	96%	0.55

B	*Polyvinyl alcohol (**5**)*	**H_2**	**CO**	**Formic Acid**	**Other**	**Total FE**	**Total Current (mA/cm^2)**
	Average	**71%**	**15.1%**	**17%**	**0%**	**103%**	**0.54**
	SEM	**2%**	**0.6%**	**1%**	**0%**	**1%**	**0.06**
	STD	**3%**	**1%**	**2%**	**0%**	**2%**	**0.1**
	Trial 1	69%	14.7%	19%	0%	103%	0.51
	Trial 2	68%	14.2%	18%	0%	100%	0.65
	Trial 3	74%	16.3%	14%	0%	105%	0.45

C	Polyethylene glycol (**6**)	**H_2**	**CO**	**Formic Acid**	**Other**	**Total FE**	**Total Current (mA/cm^2)**
	Average	**44%**	**16%**	**38%**	**0%**	**98%**	**0.70**
	SEM	**6%**	**3%**	**3%**	**0%**	**2%**	**0.08**
	STD	**13%**	**5%**	**5%**	**0%**	**3%**	**0.17**
	Trial 1	36%	19%	38%	0%	93%	0.57
	Trial 2	30%	22%	45%	0%	97%	0.54
	Trial 3	57%	11%	33%	0%	101%	0.86
	Trial 4	52%	13%	35%	0%	99%	0.83

Table S9. Data for Figure 2

Ox Cu and tetrahexadecylammonium bromide (**2**) may be found in **Table S6**.

A	Trihexyltetradecyl-phosphonium bromide (**7**)	**H_2**	**CO**	**Formic Acid**	**Other**	**Total FE**	**Total Current (mA/cm^2)**
	Average	**27%**	**49%**	**11%**	**0%**	**87%**	**0.115**

SEM	**2%**	**3%**	**2%**	**0%**	**4%**	**0.003**
STD	**4%**	**6%**	**4%**	**0%**	**8%**	**0.006**
Trial 1	22%	52%	9%	0%	84%	0.11
Trial 2	26%	50%	7%	0%	83%	0.11
Trial 3	31%	40%	12%	0%	83%	0.12
Trial 4	29%	53%	16%	0%	98%	0.12

B	Dihexadecyldimethyl-ammonium bromide (**8**)	**H_2**	**CO**	**Formic Acid**	**Other**	**Total FE**	**Total Current (A/cm^2)**
	Average	**3%**	**76%**	**18%**	**0%**	**97%**	**0.31**
	SEM	**2%**	**5%**	**4%**	**0%**	**1%**	**0.03**
	STD	**3%**	**9%**	**6%**	**0%**	**2%**	**0.06**
	Trial 1	0%	81%	14%	0%	95%	0.35
	Trial 2	1%	82%	16%	0%	99%	0.25
	Trial 3	6%	66%	25%	0%	97%	0.34

C	Didecyldimethylammonium bromide (**9**)	**H_2**	**CO**	**Formic Acid**	**Other**	**Total FE**	**Total Current (mA/cm^2)**
	Average	**21%**	**8%**	**62%**	**0%**	**91%**	**2.45**
	SEM	**3%**	**1%**	**3%**	**0%**	**2%**	**0.29**
	STD	**6%**	**2%**	**7%**	**0%**	**5%**	**0.57**
	Trial 1	19%	8%	61%	0%	89%	2.15
	Trial 2	16%	10%	71%	0%	97%	1.85
	Trial 3	29%	6%	59%	0%	93%	3.15
	Trial 4	22%	8%	57%	0%	87%	2.64

D	Cetyltrimethylammonium bromide (**10**)	**H_2**	**CO**	**Formic Acid**	**Other**	**Total FE**	**Total Current (mA/cm^2)**
	Average	**34%**	**3.64%**	**56%**	**0.08%**	**93%**	**4.17**
	SEM	**1%**	**0.05%**	**2%**	**0.05%**	**1%**	**0.15**
	STD	**2%**	**0.1%**	**3%**	**0.09%**	**2%**	**0.26**
	Trial 1	35%	3.65%	54%	0.18%	93%	3.91
	Trial 2	34%	3.55%	54%	0%	91%	4.42
	Trial 3	31%	3.72%	59%	0.07%	94%	4.17

SM. References

1. Lobaccaro, P.; Singh, M. R.; Clark, E. L.; Kwon, Y.; Bell, A. T.; Ager, J. W. Effects of Temperature and Gas-Liquid Mass Transfer on the Operation of Small Electrochemical Cells for the Quantitative Evaluation of CO_2 Reduction Electrocatalysts. *Phys. Chem. Chem. Phys.* **18**, 26777-26785 (2016).